UPTEC W 22035
Examensarbete 30 hp
2022-11-02

UPPSALA UNIVERSITET

Comparison of temperature variability and trends in Svalbard and Franz Joseph Land

Johanna Renberg

Civilingenjörsprogrammet i miljö- och vattenteknik

UPPSALA UNIVERSITET

Comparison of temperature variability and trends in Svalbard and Franz Joseph Land

Johanna Renberg

Abstract

Arctic warming is assumed to be four times the global warming. A published study by Ivanov et al. (2019) shows that the annual average temperature of Franz Joseph Land (the world's northernmost island region, a Russian territory) has increased by 5.2 °C from 2000-2017. This result supported the idea of determining whether Svalbard (Norwegian territory) is experiencing similar warming. Svalbard has historically been an attractive research center for examining climate change in the Arctic. Due to easier accessibility, the vast majority of weather stations have been located on the western part of the main island, Spitsbergen, which does not provide a representative picture of the entire archipelago. Therefore, this project has focused on eastern Spitsbergen. Data from six stations have been processed to analyze the temperature changes based on linear regression (the same method as at Franz Joseph Land). As eastern Spitsbergen has never been a priority, only short datasets are available, with the longest one dating from 2009. Because of this, no statistically significant result could be elucidated. Instead, data from Longyearbyen, which is located southwest were implemented, allowing analysis over the same period as Franz Joseph Land (2000-2017). This result suggested a temperature increase of 5.6 °C for the same period, with a statistical significance of $P = 0.13$, as well as that the winters are extra vulnerable to warming. The stations from eastern Spitsbergen's local variability were also examined, which showed that the local climate varies although the stations are relatively close. Among others, Pyramiden seemed to be most affected by the lapse rate feedback, meaning a significant strong warming at the surface.

Keywords
Arctic warming, Arctic Amplification, Franz Joseph Land climate, Svalbard climate, linear regression.

Teknisk-naturvetenskapliga fakulteten

Uppsala universitet, Utgivningsort Uppsala/Visby

Handledare: Veijo Pohjola Ämnesgranskare: Ward van Pelt

Examinator: Antonio Segalini

Referat

Uppvärmningen för Arktis antas vara fyra gånger den globala uppvärmningen. En publicerad studie av Ivanov et.al, (2019) visar att den årliga medeltemperaturen för Franz Joseph Land (världens nordligaste skärgård, ryskt territorium) har ökat med 5,2 °C under perioden 2000–2017. Detta resultat har använts som grund för att avgöra ifall Svalbard (norskt territorium) uppvisar likande uppvärmning. Svalbard har under historien varit ett attraktivt forskningscentrum för Arktisk miljö. På grund av enklare tillgänglighet har de allra flesta väderstationer blivit placerade till västra delen av huvudön, Spitsbergen, vilket inte gett en representativ bild av hela ö-landskapet. Därför har detta projekt fokuserat på östra Spitsbergen. Totalt sett har data från sex olika stationer processats för att analysera temperaturutvecklingen, som baserats på linjär regression (samma metod som för Franz Joseph Land). Då östra Spitsbergen aldrig varit prioriterad finns få tillgängliga data, med den längsta serien från år 2009. På grund av detta kunde inget statistiskt signifikant resultat klargöras. I stället implementerades data från Longyearbyen, belägen längre sydväst, vilket möjliggjorde analys under samma tidsperiod som Franz Joseph Land (2000–2017). Detta resultat tydde på en temperaturökning med 5,6 °C under samma tidsperiod, med statistisk signifikans med P = 0,13. Stationerna från östra Spitsbergens lokala variabilitet har också undersökts, som visade på att klimatet skiljer sig tydligt trots korta avstånd från varandra. Bland annat visar resultatet att stationen Pyramiden verkar vara starkt påverkad av temperaturavtagnings-återkoppling (lapse rate feedback), som innebär en stark marknära uppvärmning.

Nyckelord

Arktisk uppvärmning, Arktisk amplifiering, Franz Joseph Land klimat, Svalbard klimat, linjär regression

Preface

This thesis was written as the conclusive part of the master's program in Environmental and Water Engineering at Uppsala University, holding 30 credits. The supervisor for this project was Veijo Pohjola, professor at the Department of Earth Sciences, Program for Air, Water and Landscape Sciences; Physical Geography and subject reviewer Ward van Pelt, Senior Lecturer/Associate Professor at the same departure.

Initially, I would like to bring a big thank you to Veijo Pohjola for accepting this partnership, even though everything has been done remotely from Innsbruck, Austria, and I am so grateful for you always believing in me and pushing me in the right direction when I doubted myself. Your kind words gave me the confidence and motivation to reach my goal and finish this thesis. I also thank Ward van Pelt for helping me with Matlab problems. This is the first data analysis I have completed; your input has helped a lot. My sister, Lovisa Renberg, has also supported me throughout this process and given me much good input for improvements. Lastly, I would like to thank my family and all my friends from Uppsala and Innsbruck for supporting me through this project and making my study years as good as they have been. I have so many unforgettable memories. Thank you all!

Johanna Renberg,
Uppsala, 2022.

Populärvetenskaplig sammanfattning

För en tid sedan publicerades en studie som visar att Arktis utsätts för uppvärmning fyra gånger det globala medelvärdet. Under 2019 publicerads en annan studie, utförd av Ivanov et.al, som undersökte klimatförändringar på världens nordligaste skärgård, Franz Joseph Land. Ett av deras resultat var att medeltemperaturen för Franz Joseph Land har under perioden 2000–2017 ökat med hela 5,2 °C. Detta var och är ett oroväckande resultat, samt anledningen till att jag velat undersöka ifall liknande temperaturökning har skett i andra delar av Arktis, närmare bestämt Svalbard.

Svalbard har länge varit en utmärkt plats att för att forska Arktiska miljöer på eftersom det är så pass tillgängligt. När forskare förr i tiden placerade ut väderstationer prioriterades de till den västra delen av den stora huvudön, Spitsbergen. Detta har bidragit till att man än idag inte har en fullständig bild av hur klimatet ser ut för hela ö-landskapet. På grund av detta har jag valt att basera min undersökning till den östra delen av Spitsbergen. Totalt sätt har väderdata från sex olika stationer används och på grund av relativt ny stationering sträcker sig data inte längre bak än år 2009.

För att möjliggöra en jämförelse med resultatet från Franz Joseph Land har det varit viktigt att använda samma tillvägagångssätt. Ivanov et.al., använde en metod som kallas ”linjär regression”, som kortfattat utgår från att försöka anpassa en rak linje över den data man har. Lutningen på denna linje, som beräknades enligt den ”räta linjens ekvation”, beskriver hur mycket temperaturen har förändrats över tid. Uppåtgående lutning innebär uppvärmning och nedåtgående lutning innebär det nedkylning.

Det visade sig att när man utför en linjär regression på dessa korta dataserier från östra Spitsbergen gavs inget trovärdigt resultat. Huvudsyftet med detta arbete var att svara på ifall det går att påvisa likande uppvärmning för Svalbard som för Franz Joseph Land, så därför gjordes en ny undersökning. Vid denna nya användes data från mätstationen i Longyearbyen. Den är belägen längre sydväst och har betydligt längre dataserier. Med hjälp av denna data blev det möjligt att visa att den årliga medeltemperaturen har stigit 5,6 °C under samma tidsperiod, 2000–2017.

Eftersom arbetet fokuserade på klimatet för östra Spitsbergen, analyserades olika meteorologiska parametrar. Resultatet visar på att mätstationens placering har stor betydelse när det kommer till dess temperatur och temperaturförändringar. Bland annat verkar stationen Pyramiden utsättas för extra stor uppvärmning på grund av ”temperaturavtagnings-återkoppling” (lapse rate feedback). Det är en typisk meteorologisk process som sker i Arktis, och som påskyndar uppvärmningen.

Table of contents

1. Introduction

Arctic regions have shown a four times stronger response to global warming than the global average (Rantanen et al., 2022). This is called Arctic amplification and is a result from amplified climatic feedback with consequences like sea-level rise, permafrost changes, ice sheet melting, see section 3.2. This arctic warming is expected to continue even in the coming decades (Hanssen-Bauer et al., 2019).

Svalbard, the world's northernmost urban community, is a proper place for scientists to study global warming in an Arctic climate. Svalbard is a Norwegian territory surrounded by the Norwegian sea to the west and The Barents Sea to the east. Due to its easy accessibility, meteorological data have been collected since 1898 Nordli et al. (2020). However, these long-term measurements are primarily located in the archipelago's western part. Other regions, such as the eastern parts, have never been prioritized. The longest measured meteorological data series in these eastern regions goes back to 2009, resulting that its regional climate is still relatively unknown. Northeast of Svalbard lies another Russian archipelago, Franz Joseph Land. Due to the inaccessibility and the lack of longer homogeneous climate series, only a few climate studies have been performed in this region. But in 2019, Ivanov et al. studied the long-term change in the surface air temperature from 1929 to 2017 by combining shorter data sets from two measurement sites. Results showed, among others, that the temperature for the entire period has increased by 1.6 – 1.8 °C, and for the latest period (2000-2017) the temperature has increased up to 5.2 °C. This study will use the results from Franz Joseph Land and see if comparable results in the eastern part of Svalbard can be obtained.

2. Aims and objectives

This study will analyze climate changes in the eastern part of Spitsbergen. This is performed by comparing the increasing temperature on Franz Joseph Land with data from six meteorological stations from Svalbard. I will further analyze a wider range of meteorological parameters (surface air pressure, relative humidity, windspeed, short- and long-wave in-, and outgoing radiation) to understand why these temperature changes occur. The local variability will be investigated, the importance of its position when examining climate changes, and which parameter co-varies with the temperature increase to analyze which local processes are driving the amplification.

The questions I will investigate are:

1. How have the surface air temperatures changed on the eastern Spitsbergen during the last decade? Are the results comparable to changes on Franz Joseph Land?

2. What is the local variability of the six weather stations on eastern Spitsbergen, and how does the topographical setting influence the temperature at these stations?

3. Can local temperature variations be linked to changes in other weather variables?

3. Background

3.1 Svalbard

Svalbard, the Norwegian archipelago in the Arctic Ocean, is located between longitude 10° and 35° E and latitude 74° and 81° N (Britannica., 2022), with an area of around 61 500 km^2. The archipelago includes eight islands. The larger ones are Spitsbergen (39 000 km^2), Nordaustlandet (14 600 km2), Edgeøya (5 000 km2), and Barentsøya (1 300 km2). The smaller and more isolated ones are Prins Karls Foreland, Kvitøya, Kong Karls Land, Bjørnøya, and Hopen (Nationalencyklopedin, n.d.) (see Figure 1).

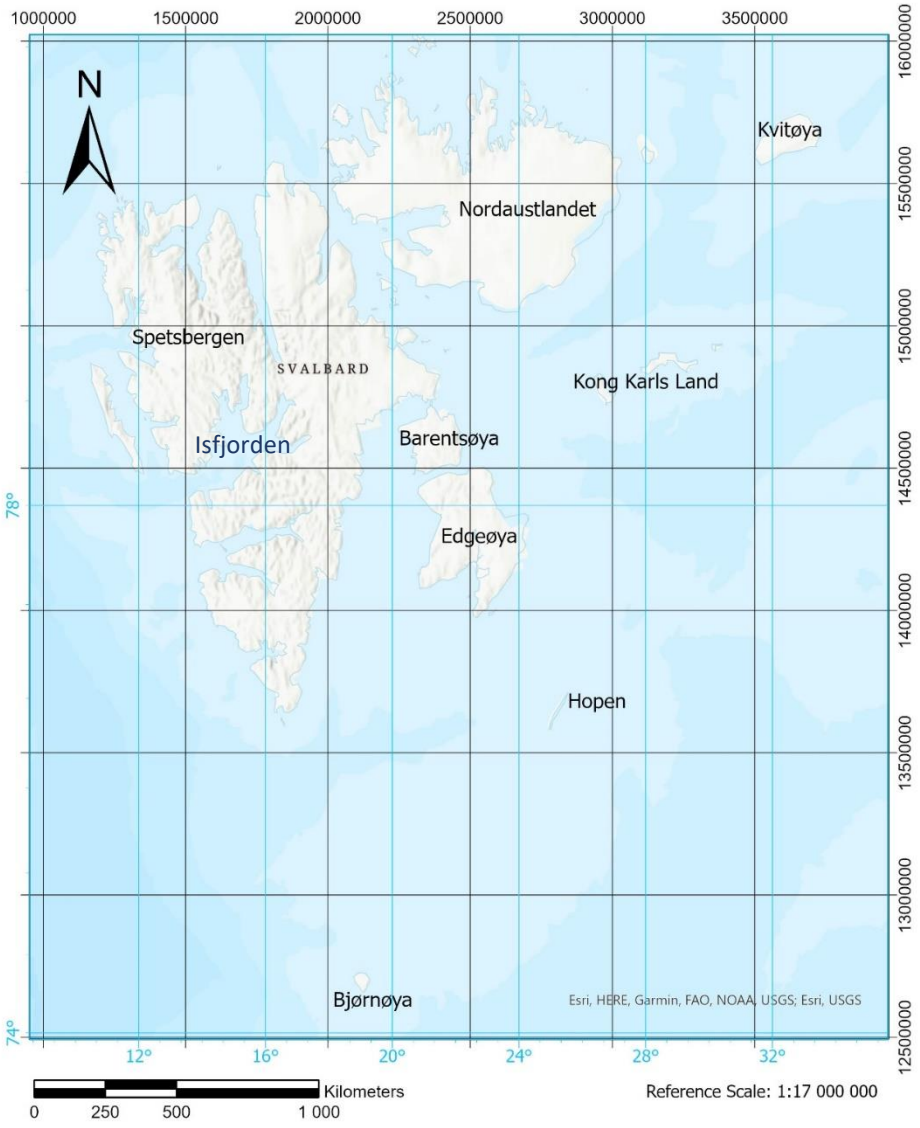

Figure 1. An overall map over the Svalbard archipelago.

Due to its high latitude and climate, around 60 % of Svalbard's total land area is covered by snow and ice and has more than 2,100 glaciers (Pandit, 2021). The topography is strongly influenced by the Pleistocene glacial, and the accompanying land uplift, resulting in numerous fjords along the northern and western coastlines. One of the largest ones is Isfjorden which reaches into the center of Spitsbergen. Since the area is above the Arctic circle, the region has

a typical Arctic climate. The monthly mean temperature usually does not exceed 10 °C, and trees and forests do not grow on Svalbard (Nationalencyklopedin, n.d.). During summertime (April 20 to August 23), the sun never sets, and during wintertime (October 26 to February 15), the sun never rises (Norska Polarinstitutet, n.d.).

Svalbard was discovered in 1596 during an expedition by the Dutchman Willem Barents. However, it is believed that Icelandic seafarers may have found the archipelago as early as AD 1194. Svalbard was inhabited by whalers, fishermen, and fur hunters from various countries in the following centuries. Around year 1900, the exploitation of large coal deposits began and at the year of 1925, the archipelago became an official belonging to Norway. Hence, the Soviets still had rights to continue their coal mines. After World War II, in 1941, Svalbard changed significantly after the allied and the axis powers of the war destroyed installations to make warfare more difficult for the other side. The population was evacuated, the coal mines were taken out of operation, and much was destroyed. After the war, the Soviets demanded to participate and share the island territory with Norway. As a result, Norwegian and Soviet mining operations resumed and are still in operation (Nationalencyklopedin, n.d.)

Besides the valuable coal mining, Svalbard is and has for long been an important place for scientists to study the Arctic, mainly because of its easy accessibility. The first weather station was established in 1898 (Nordli et al. 2020)., and several other meteorological stations have been positioned since then. The first stations were mainly situated along the western coastline of Spitsbergen, which has led to that the local climate for the entire Spitsbergen interior and surrounding islands being relatively unknown. Hanssen-Bauer et al. (2019) tried to get an overall view of the spatial temperature over the archipelago. They produced Figure 2, showing that the temperature varies greatly depending on the location. The southwestern parts tend to be considerably warmer than the northeastern parts. The colder temperatures are a consequence of the cold air masses from the northeast, and the warmer temperatures are a consequence of the warmer air masses from the West Spitsbergen Current that runs along the west coast. More about this is in section 3.3. Even if Figure 2 shows various spatial temperatures over Svalbard, these results are from a model and not real measured values. The eastern Spitsbergen has never been prioritized since it is further away from civilization and has a more challenging topography, which has led to a lack of longer homogeneous representative datasets for these areas (Hanssen-Bauer et al., 2019).

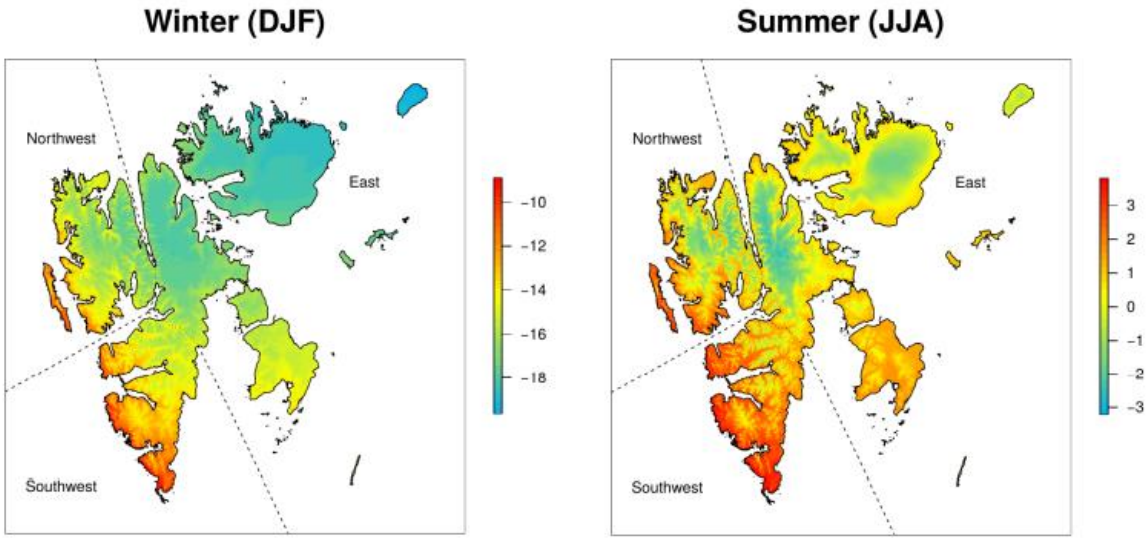

Figure 2. The average temperature (°C) over 1971-2000 for the winter months (Dec-Jan-Feb; left) and summer (Jun-Jul-Aug; right). Notice that the scales are different (Hanssen-Bauer et al., 2019).

3.2 Franz Joseph Land

Northeast of Svalbard lies another archipelago, Franz Joseph Land. It is governed by Russia and is the world´s northernmost archipelago, containing 192 islands on an area of around 16.000 km^2. It is an uninhabited island chain and has, for an extended period, been fully covered by ice (National Geographic Society, 2013). Only a few weather stations are situated in this region, due to the inaccessibility. Franz Joseph Land has so far not been of high interest to researchers, so published scientific results with homogeneous and accurate data series only cover the period from 1958 to 1995. Observations before and after this period are irregular and inaccurate (Ivanov et al., 2017). Long-term homogeneous series are essential when assessing climate change for evaluating trends and estimating spatial and temporal scales. To achieve this, Ivanov et al. (2017) created a homogeneous series of the monthly average surface air temperature with available data from Russian instrumental observations, Bukhta Tikhaya and Krenkel Observatory, from 1929 to 2017. Their results have given a more extensive understanding of temperature changes for Franz Joseph Land and have make it possible to compare results with other parts of the Arctic. In this case, Svalbard.

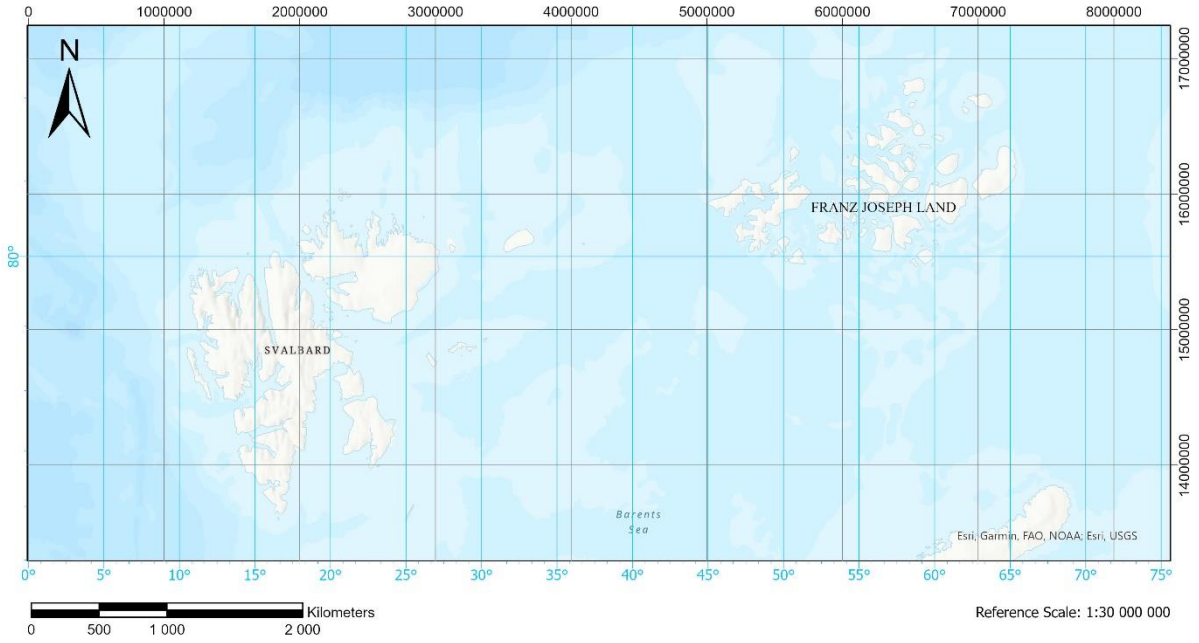

Figure 3. The relation between Svalbard and Franz Joseph Land.

3.3 Oceanic currents and The Barents Sea

The regional climates of these two Arctic archipelagos are strongly linked to the large-scale circulation between the North Atlantic and the Arctic Ocean (Hanssen-Bauer et al., 2019). Figure 4 shows how the Atlantic water masses from the Gulf Stream flow northwards, bringing salt and warm water (red arrows). At the break of the continental shelf, this current splits into two branches, with the western branch continuing along the west coast of Svalbard and is referred to as the West Spitsbergen Current, while the eastern branch continues into the Barents Sea. In the Barents Sea, the warm and saline Atlantic waters meet the colder and less saline Arctic waters of the East Icelandic Current flowing in from the southwest (blue arrows). This breaking point is called the polar front (white line), and is defined as the zone where these two currents meet, and their water masses stratify. Cold Atlantic waters sink and flow along the bottom towards the Arctic Ocean, while the colder Arctic waters flow along the surface. This means that the warmer water does not make close contact with the sea ice preventing large-scale melting along the way as the Atlantic water flows northwards towards the Arctic (ibid).

The Barents Sea only covers around 10 % of the Arctic Ocean, with an approximate volume of 1.4 million km^3 and an average depth of 230 m. However, it still plays a vital role on a larger scale for the entire Arctic and the other oceans. The Barents Sea creates an intense heat exchange between the atmosphere and the sea, creating variability in the Arctic air-ice-ocean system (Smedsrud et al., 2013).

The inflow of warm Atlantic water into the Barents Sea creates a temperature gradient between the cold atmospheric air. The resulting heat exchange contributes to melting the Arctic Sea ice cover and enhancing the surface air temperature. Exceptionally high impact occurs during winter since the warmer temperature increases the gradient to the freezing point. The greater the temperature gradient, the less ice cover freezes during the winter. The heat exchange between the surface and the surrounding atmosphere grows with an open ocean and intensifies

warming. Calculations have shown that by 2050 the Barents Sea is expected to be ice-free all year round (Smedsrud et al., 2013).

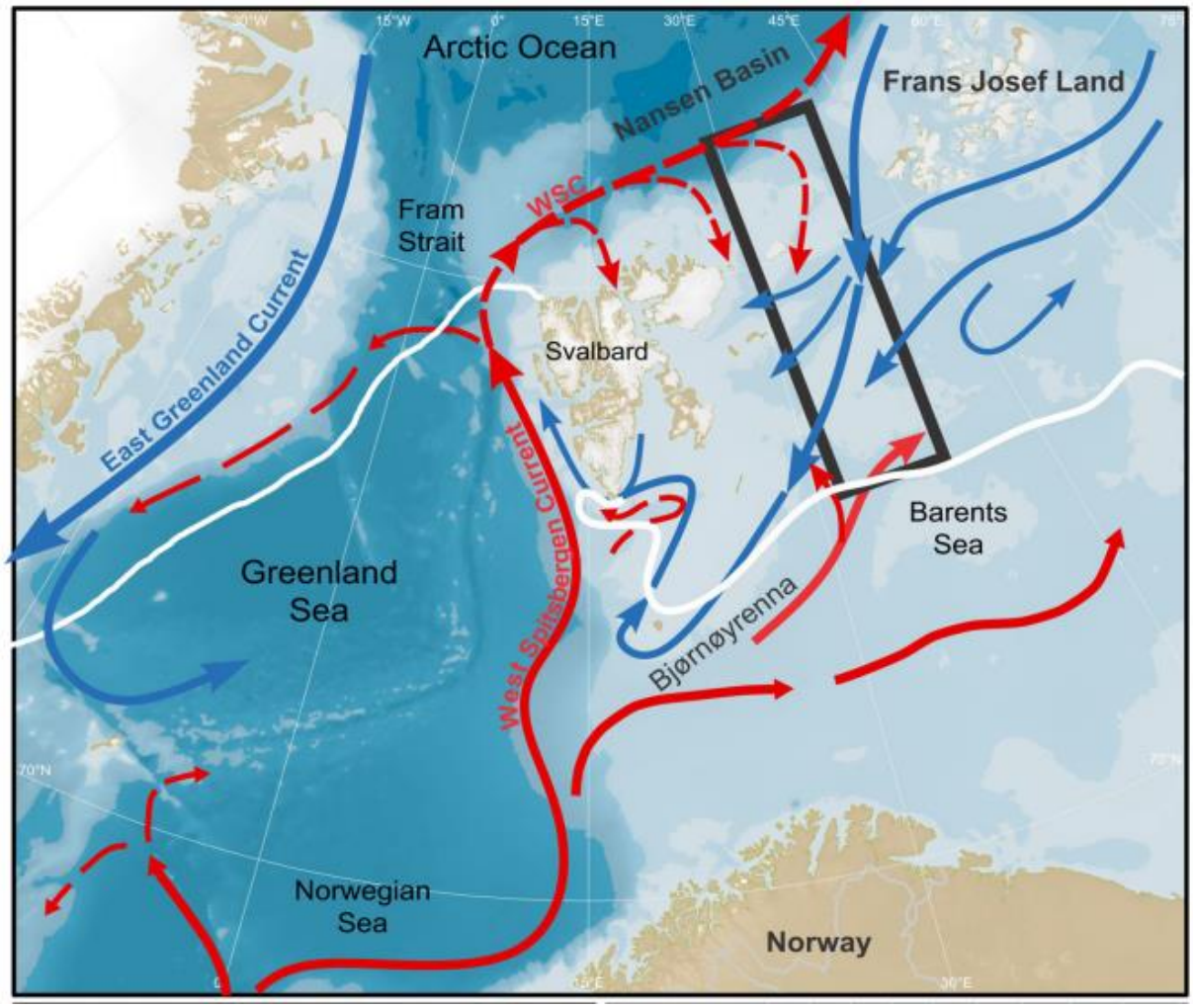

Figure 4. The oceanic currents around Svalbard. Red arrows correspond the saline and warmer Atlantic water masses from the Gulf Stream in a northward's direction. At the break of the continental shelf, the currents split into the western branch, the West Spitsbergen Current and the eastern into the Barents Sea. The blue arrows correspond to the colder and less saline water with the Icelandic Current. The breaking point between these water masses is called the polar front (white line) (Zamelczyk et.al, 2021).

3.4 Arctic amplification and climate feedback

Arctic regions closer to the poles have over time tended to show a significantly stronger response to global climate forcing than the rest of the globe. This phenomenon is known as Arctic amplification (Hanssen-Bauer et al., 2019). Amplified warming and cooling have occurred throughout the past three million years and are proven by annual surface air temperature trends (Serreze, M. C., & Barry, R. G., 2011). For the last 43 years, a significant increase in temperature has been apparent. A recent study published in August 2022, made by Rantanen et al., (2022) indicates an annual mean temperature warming for the Arctic regions (60°N–90°N) up to four times greater than the global mean.

The main reason for this is partly linked to climate feedback. The term "climate feedback" refers to when the effect of climate processes either amplifies or dampens the initial climate

response. An amplified response is denoted as positive feedback, and a dampened response represents negative feedback (Serreze, M. C., & Barry, R. G., 2011). There are numerous climate feedback processes, but the most dominant ones in the Arctic are Planck feedback, albedo feedback, and lapse rate feedback.

3.4.1 Planck feedback

The most basic and universal one is the Planck feedback. Briefly, the Planck feedback describes how the earth tries to even out the incoming global radiation to reach a warming equilibrium, leading to differently distributed outgoing longwave radiation. Around the equator, with a greater solar angle, most energy emits out; meanwhile, at the poles, with a lesser solar angle, the outgoing radiation is the smallest. In other words, colder areas store more energy, as Cronin, T. W. (2020) describes it: "Planck feedback is the rate of increase of infrared energy loss per unit vertically." Due to its location close to the north pole, Svalbard is constantly affected by the positive Planck feedback without any external influence (Hanssen-Bauer et al., 2019 & Previd et al., 2021)

3.4.2 Albedo feedback

When the highly reflective snow and ice covers melt, more significant parts of darker, less reflective areas absorb solar energy more efficiently, enhancing the warming processes. The retreat of sea ice is particularly sensitive since it can cause large-scale changes and give rise to other feedback processes. For example, when larger sea ice sheets in the Arctic oceans retreat, the vertical heat fluxes between the ocean and atmosphere change, so water vapor content variations occur, which affects the cloud cover that changes longwave radiation fluxes, etcetera. (Serreze, M. C., & Barry, R. G., 2011). The albedo feedback argues being the second largest contributor to amplified warming in Arctic regions (Hanssen-Bauer et al., 2019).

3.4.3 Lapse rate feedback

When an air parcel rises in the atmosphere, the air parcel expands because of reduced pressure. With this expansion, the temperature of the air parcel drops, and the rate at which this air parcel temperature drops are referred to as the "*dry adiabatic lapse rate"*. The term "adiabatic" assumes the air parcel to be entirely thermally insulated from its surrounding air and is calculated according to Equation 1. In dry air, the air parcel temperature decreases by around 10 °C per 1000 meters (Laurin et al., n.d. & Hemond, H. F., & Fechner, E. J., 2015).

$$\Gamma_{dry} = -\frac{dT}{dz} = -9{,}8\ ℃/km \qquad \text{(Eq. 1)}$$

The air is mostly humid, which affects the vertical temperature decrease. When a saturated parcel expands and cools down, the water will first condense. This process releases latent heat, which delays the cooling. The "*moist-adiabatic lapse rate*" is therefore lowered to around 4 °C to 7 °C for every 1000 m, depending on humidity (ibid).

The vertical air movements also depend on atmospheric stability. Under *neutral stratification*, the air parcel temperature decreases by 10 °C per 1000 meters. In *unstable stratification*, the temperature decreases by more than 10 °C per 1000 meters, and vertical motion is facilitated. Conversely, in a *stable stratification*, the temperature gradient is less than 10 °C per 1000 meters, which prevents vertical movements (SMHI, 2022).

The climate is usually cold and dry in the Arctic regions. Hence, the atmosphere generally has stable stratification conditions in the lower troposphere, indicating a temperature increase with altitude (Boeke et.al., 2020). However, this is not true for Svalbard. Svalbard is considerably milder, wetter, and cloudier than the average for this latitude. This is due to the transition zone of air masses over the archipelago, where cold Arctic air in the north encounters the mild, marine, and humid air in the south, following along the West Spitsbergen Current. This leads to unstable and stormy weather resulting in numerous cyclones, especially during the winter (Hanssen-Bauer et al., 2019). This results in various atmospheric stratification for the archipelago, where the lapse rate typically follows a *moist-adiabatic lapse rate*.

The temperature gradient between the surface and the atmosphere is dependent on the atmospheric stratification and will vary. When the atmosphere has stable stratification, the released heat from the ground will have difficulties mixing with the air masses in the atmospheric layers above (up to 5000m), which means a more intensified warming at the surface, resulting in a positive lapse rate feedback (Hanssen-Bauer et al., 2019). In Arctic regions, this lapse rate feedback is argued to be the most significant contributor to amplified warming (Boeke et.al., 2020.; Hanssen-Bauer et al., 2019).

There is strong evidence that the Arctic amplification will continue to develop and extend its impact ahead of the Arctic. A warmer mean temperature invokes changes in the atmospheric circulation, which later risk impacting areas outside the Arctic regions (Serreze, M. C., & Barry, R. G., 2011).

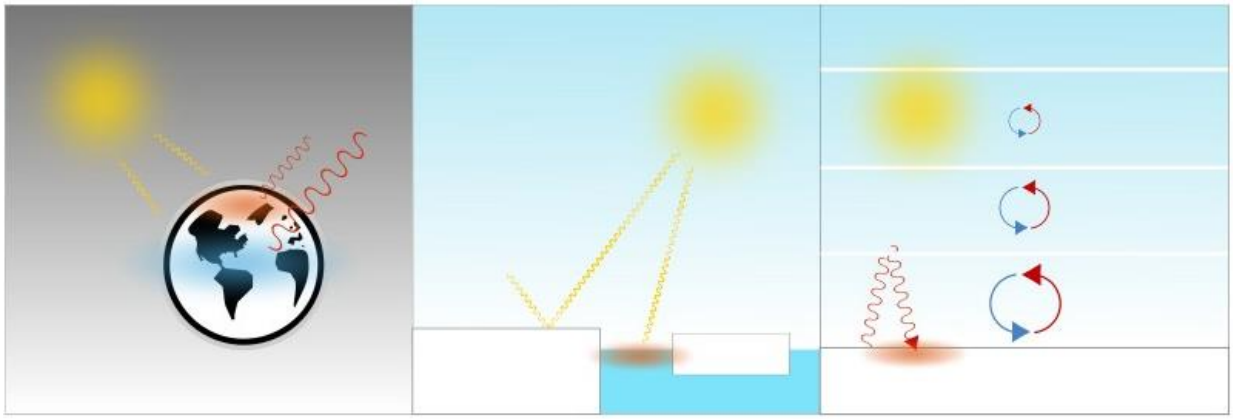

Figure 5. The left once visualizes "the Planck feedback". The poles store more energy compared to the equator. The middle shows "the Albedo feedback". When sea ice is melting, the solar radiation will heat up more water which increases the temperature. The right one is "the lapse rate feedback". The atmosphere gets stratified that prevents vertical air motion, which traps the warmer air that gets transmitted from the ground.

4. Data acquisition

The data used from eastern Spitsbergen have been downloaded online from *Svalbard Integrated Arctic Earth Observing System* (SIOS). Data for Franz Joseph Land have been collected from their report (Ivanov. et al., 2017) and online from the *All-Russian Scientific Research Institute of Hydrometeorological Information - World Data Center (VNIIGMI-WDC).* The data series from eastern Spitsbergen are very short, with the longest one only starting in 2009. To have a data series longer than that, data from Longyearbyen (the main city of Svalbard) have been downloaded.

4.1 Meteorological stations on Svalbard

- **Pyramiden (PY)**
  The station is an abandoned Russian coal mining settlement and is now owned by the Norwegian Meteorological Institute. The station is located 250 m from the shoreline of the Isfjorden and has a height of 20 m.a.s.l.

- **Ulvebreen (UB)**
  The dataset is provided by Dr. Carleen Reijmer from Utrecht University and has data with hourly values. It is located close to the Ulvebreen tidewater glacier, at 140 m.a.s.l., and 2 km from the Barents Sea.

- **Svenbreen (SB)**
  Data is provided by Dr. Jakub Malecki from the Adam Mickiewicz University, with a 1-day resolution. The station is close to a tidewater glacier, within a 3 km distance of Isfjorden, and at the height of 355 m.a.s.l.

- **Nordenskiöldbreen (NB)**
  The dataset is also given by Dr. Carleen Reijmer. It is stationed close to a tidewater glacier, at 530 m.a.s.l., and 4 km from the Isfjorden. The recordings are between 2009-2020, but due to problems with moisture in the sensors, the summers of 2009, 2010, 2011, and 2012 are missing (Van Pelt et al., 2012 & Van Pelt et al., 2019). The data was reconstructed, but even after the reconstruction, the dataset still included some longer gaps and NaN-values. Since the gaps are out of interest, the time interval chosen for this project is between 03/2009–03/2019.

- **Lomonosovfonna PFA (LF PFA)**
  This station is on the Lomonosovfonna glacier, 1144 m.a.s.l. This implies that the ground is constantly covered with snow all year round. The dataset is provided by Dr. Sergey Marchenko from Uppsala University has a record from 04/2018 to 05/2020, with 2 hours of time resolution.

- **Lomonosovfonna 1200 (LF 1200)**
  This station is also on the Lomonosovfonna glacier, but at a higher elevation of 1200 m.a.s.l, which means constant snow cover. Data is also provided by Dr. Sergey Marchenko with a three-hour resolution (Marchenko et al. 2016 & Marchenko et al.

2017). It has a lot of gaps and NaN-values, which is due to harsh weather conditions resulting in riming of ice on the sensors, and power outage at such a high altitude. Because of the high number of errors over a relatively short period, a reconstruction of the dataset will not be performed.

- **Longyearbyen (LYB)**
  This station is located at the Airport of Svalbard in Longyearbyen, the central city of the archipelago where most people live. It is on an elevation of 28 m.a.s.l and started its temperature recording in 1975 (Nordli et al., 2020 & Fröland et al., 2011). Only temperature data between 2000-2017 will be of interest for this thesis.

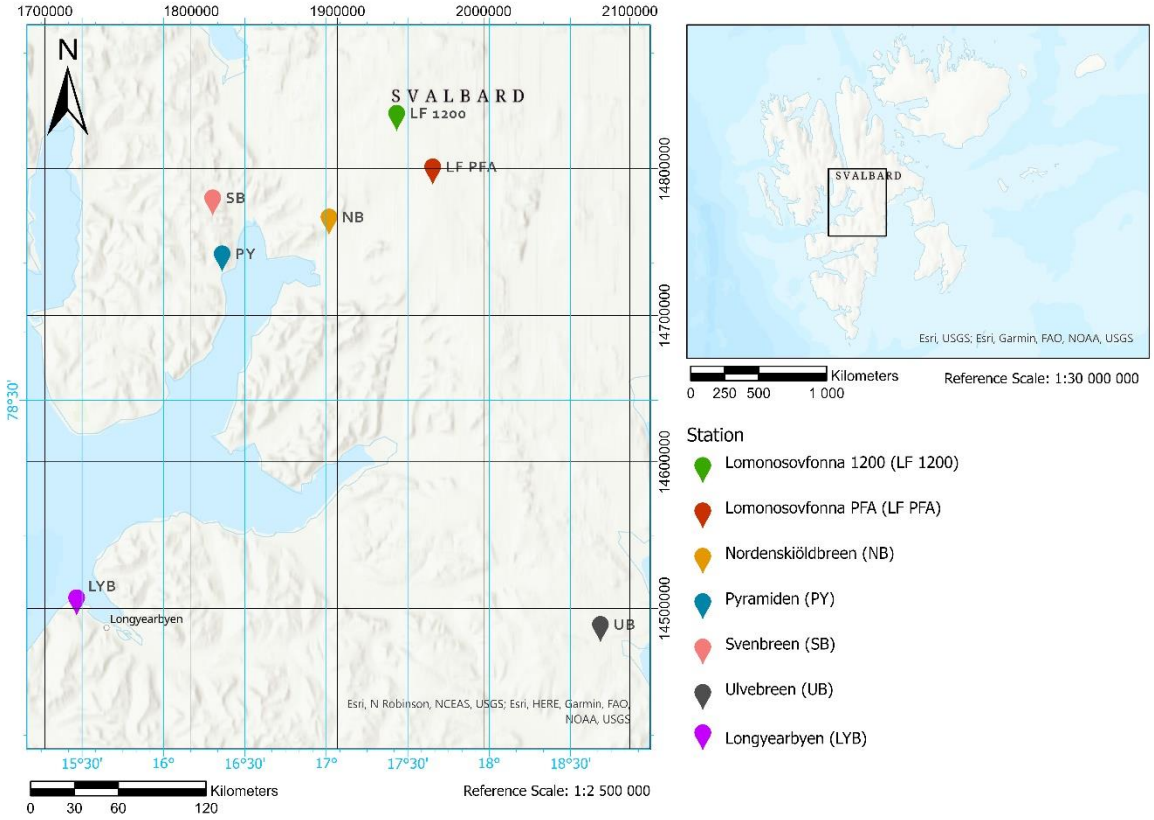

Figure 6. All meteorological stations from Svalbard. Longyearbyen (purple) is the extra one that do not count as the "easters Spitsbergen". Note that Ulvebreen is located close to the Barents Sea to the east compared to the others that are all relatively close to each other.

4.2 Meteorological stations on Franz Joseph Land

The data from Franz Joseph Land is a combination of surface air temperature series from two different meteorological stations, Bukhta Tikhaya and Krenkel Observatory, see Figure 7. The measuring period started in 1929 and is still up and running. These stations were the only ones located in the northern part of the Barents Sea during this period. However, Bukhta Tikhaya was taken down in 1960, leading to the Krenkel Observatory being the only operating meteorological station for Franz Joseph Land (Ivanov et al., 2017).

The data set from Bukhta Tikhaya covers the period from September 1st, 1929, until February 29th, 1960. It was located on Hooker Island in the southwestern part of the archipelago (80° 20' N, 52° 46' E), with an elevation of 5.9 m.a.s.l. Since the start, its location has been relocated

vertically two times. At first, in September 1932, the site got a new elevation of 8.4 m.a.s.l, then in July 1959, to a height of 16.2 m.a.s.l (ibid). Observations for the second meteorological station, Krenkel Observatory, began on November 1st, 1957, until today. The dataset includes one longer break between 2001 and 2004 due to a fire. The site is in the central part of the archipelago (80° 37' N, 58° 03' E) and has an elevation of 21 m.a.s.l (ibid).

The stations have an approximate distance of 100 km from each other. The main difference in temperature regime is that regions around Hayes Island are covered by stable land-fast ice during wintertime, and parts around Hooker Island are enclosed by a stationary polynya (areas of open water surrounded by sea ice). The southern region of the archipelago is during summertime affected by the adjacent waters of the northern part of the Barents Sea. That is why drifting ice can be observed in the central parts of the archipelago (ibid). Nevertheless, according to Ivanov et al. (2019), the atmospheric conditions are considered equal.

In their study, these two data sets were combined into one longer homogenous series, averaging daily mean temperature values from 1929 to 2017, with reconstructed data for the gap between 2001-to and 2004. This period was divided into three different sections and the latest one was between 2000-2017. The results for this study are based on this same period and is the time interval that will be used.

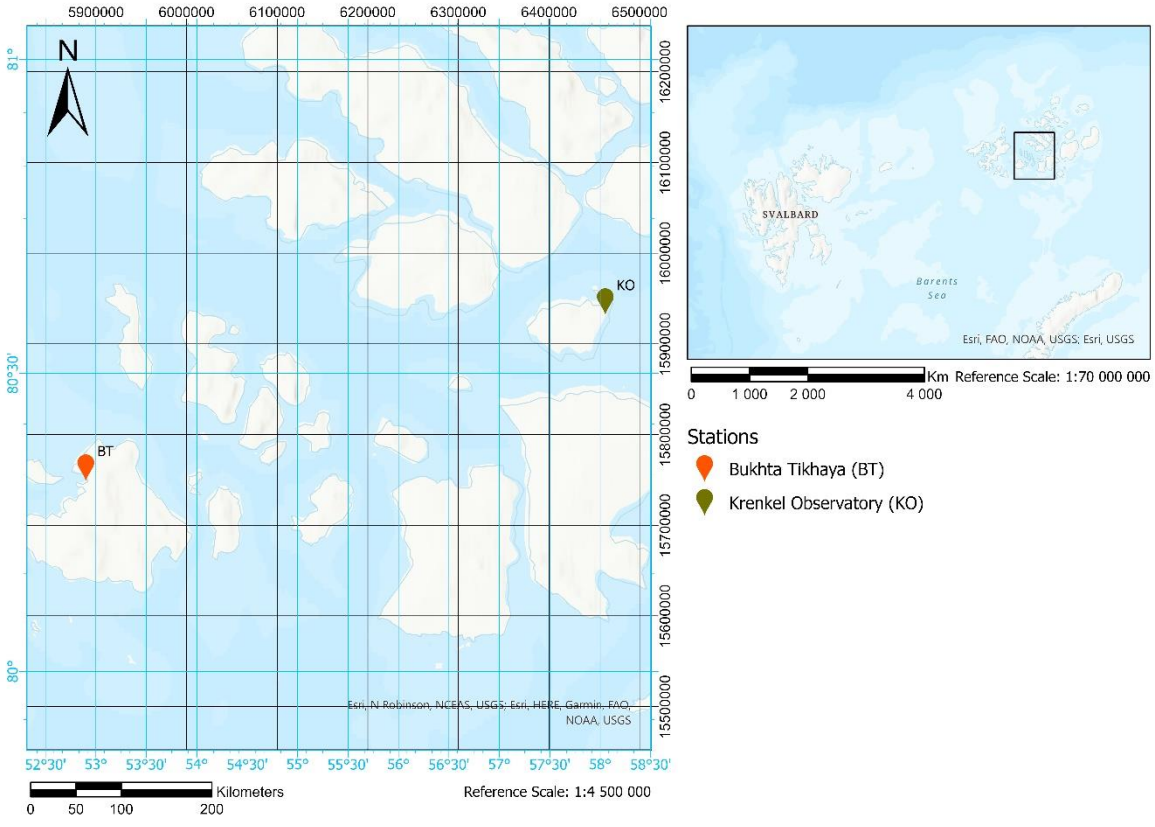

Figure 7. The two stations from Franz Joseph Land. For this study, only data from Krenkel Observatory have been used.

Table 1. All stations and their corresponding information.

	Stations	Coordinates (dd)		Measuring time	Tot years	Resolution	m a.s.l
Eastern Spitsbergen	Pyramiden (PY)	78.6557 N	16.3603 E	12/2012 - 09/2019	7	1 h	20
	Ulvebreen (UB)	78.2023 N	18.6708 E	01/2015 - 06/2020	5	1 h	140
	Svenbreen (SB)	78.7230 N	16.3020 E	09/2011 - 09/2019	8	1 h	355
	Nordenskiöldbreen (NB)	78.6667 N	17.1667 E	03/2009 – 03/2019	5	1 h	530
	Lomonosovfonna PFA (LF PFA)	78.7601 N	17.6533 E	04/2018 - 05/2020	2	2 h	1144
	Lomonosovfonna 1200 (LF 1200)	78.8240 N	17.4320 E	04/2013 - 04/2019	6	3 h	1200
	Longyearbyen (LYB)	78.2500 N	15.4667 E	01/2000 - 12/2017	17	1 day	28
Franz Joseph Land	Bukhta Tikhaya	80.3333 N	52.7667 E	09/1929 - 02/1960	31	1h	5,9 - 16,2
	Krenkel Observatory	80.6167 N	58.0500 E	11/1957 - 12/2017	60	1h	21
	FJL series for this study	-	-	01/2000 - 12/2017	17	1h	-

Table 2. All stations and their measured parameters.

		Parameters					
	Stations	Temperature (°C)	Surface air pressure (hPa)	Relative humidity (%)	Wind speed (m/s)	Short wave in/out (W/m^2)	Long wave in/out (W/m^2)
Eastern Spitsbergen	Pyramiden (PY)	Yes	Yes	Yes	Yes	No	No
	Ulvebreen (UB)	Yes	Yes	Yes	Yes	Yes	Yes
	Svenbreen (SB)	Yes	No	Yes	Yes	Yes	No
	Nordenskiöldbreen (NB)	Yes	Yes	Yes	Yes	Yes	Yes
	Lomonosovfonna PFA (LF PFA)	Yes	No	No	No	No	No
	Lomonosovfonna 1200 (LF 1200)	Yes	Yes	Yes	No	Yes	Yes
	Longyearbyen (LYB)	Yes	No	No	No	No	No
Franz Joseph Land	Bukhta Tikhaya	Yes	No	No	No	No	No
	Krenkel Observatory	Yes	No	No	No	No	No
	FJL series for this study	Yes	No	No	No	No	No

5. Methodology

5.1 Data process

The raw data from eastern Spitsbergen was incoherent, with many gaps and, in some cases, data losses for extended periods. In order to use the data, it has been necessary to process it further.

The data processing was performed in Matlab, where the first step was to remove all NaN-values (not a number) and obvious outliers from the data series to avoid possible miscalculations in the coming stages. Then, the daily average of the existing measurements for each day was calculated. Finally, due to large variability in the data records, an averaging filter was added to smooth out the trends and simplify the visualization of changes over time.

However, the available periods for each station were not the same. Figure 8 pictures their existing series as well as gaps of data along a time axis. Longer gaps exist for Lomonosovfonna 1200 and Nordenskiöldbreen, and a reconstructed gap for Franz Joseph Land.

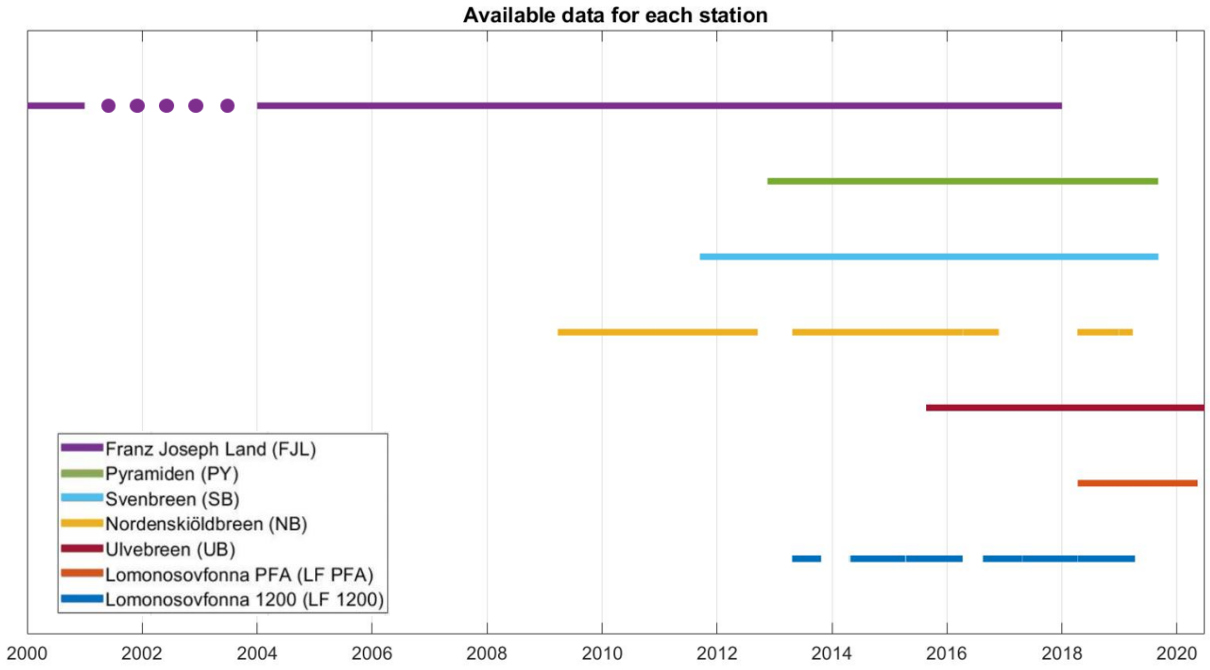

Figure 8. The available data for all stations. Note that Franz Joseph Land has reconstructed data for its gaps (purple dots). Nordenskiöldbreen and Lomonosovfonna 1200 still include gaps in the dataset.

5.2 Gaussian filter

A Gaussian filter was chosen to improve the trend's visibility. Gaussian filtering is based on a smoothing method with a Gaussian kernel, which has a shape of a normal distribution curve and is calculated according to Equation 2 (Brett, 2016 & Regmi, 2021). The advantage of this method is that the filtered value will be influenced by its neighboring values differently depending on the distance from its real value. The neighboring values closer to the real value will be weighed stronger (maximum 1). Meanwhile, neighboring values further away will be weighed less (minimum 0). The number of impacting neighboring values depends on the kernel's σ value (standard deviation). A smaller σ implies fewer neighboring values, but the closest one has the most significant impact. Meanwhile, a larger σ indicates more neighboring values, but they all impact more—the larger the σ, the smoother the data. Figure 9 illustrates how an added kernel with two different σ values encloses a different number of neighboring values. As seen, the smaller σ (pink) generated a peakier distribution curve which means that fewer neighboring values will impact the filtered value and the resulting trend is less smoothed. The larger σ (blue) generated a wider distribution curve, so more neighboring values will impact the filtered value and the resulting trend will become more smoothed. The filtered value will be the ratio between the mean sum of the kernel function multiplied by the real values. Each value for the entire dataset will have an individual calculated kernel.

$$Filterd\ value = \frac{\sum_{i=1}^{n} K(x, x_i)x}{\sum_{i=1}^{n} K(x, x_i)} \qquad \text{Eq. (2)}$$

$$K(x, x_i) = \exp\left(-\frac{(x - x_i)^2}{2\sigma^2}\right)$$

Where K is the Kernel, x is its actual value, x_i is the position of the center of the gaussian curve, and σ is the standard deviation.

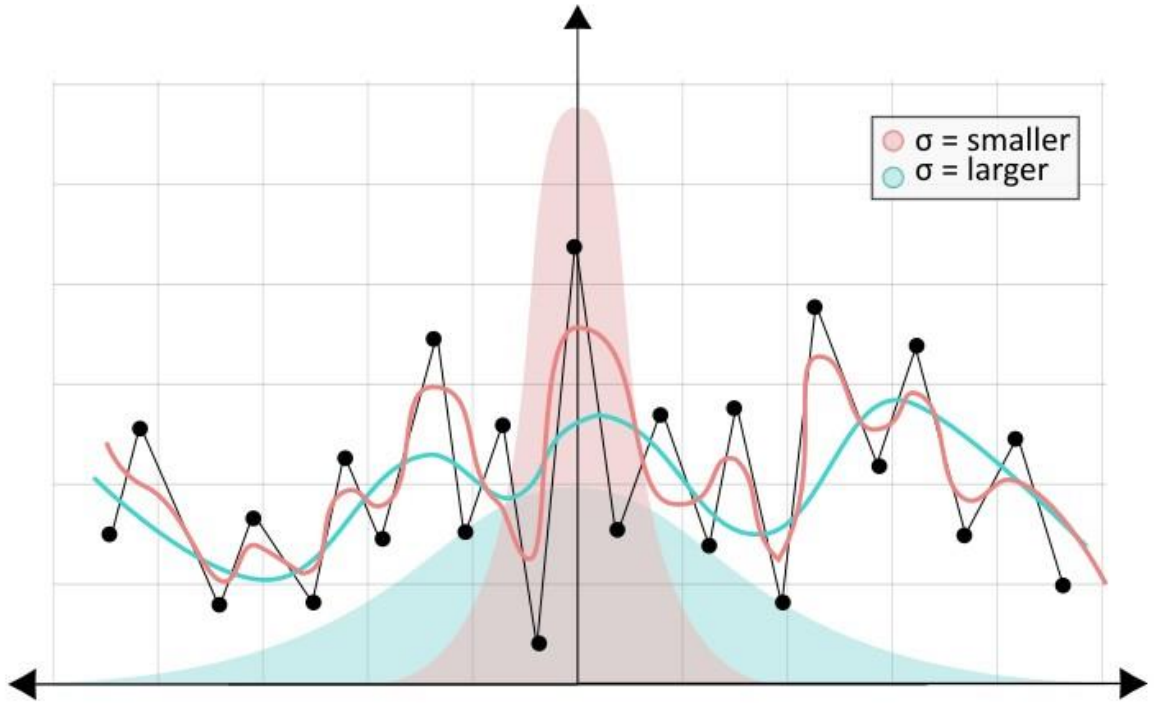

Figure 9. An illustration of how a dataset is affected by two different σ values. A smaller σ encloses fewer neighboring values (pink) and has a less smoothed trend. A larger σ encloses more neighboring values (blue) and has a more smoothed trend.

5.3 Linear regression for temperature changes

This study compares temperature changes over time between eastern Spitsbergen and Franz Joseph Land. It is vital to use an equal analyzing method, so the strategy is replicated from Ivanov et al.´s method.

At first, the monthly temperature averages over the entire data set were calculated, and all the monthly values were grouped. Linear regression was fitted for each set of months to see how the temperature changed that month, year by year (see example in Figure 10). The data sets from Nordenskiöldbreen and Lomonfovnnova 1200 included gaps. Hence, their linear regression is only based on inclusive data, leading to a less reliable result. The *a*-coefficient describes the slope angle, and the greater the positive *a*-coefficient, the greater the temperature change for that month over the specified time interval. The associated regression coefficient R^2

and *P*-value (from the calculated t-test) are also summarized in a shared table. R^2 describes how the points along the line depend on each other. The greater the R^2, the more dependent they are (Sundell, 2019). The *P*-value indicates the statistical significance between the points along the line. For example, if the $P < 0{,}25$ for a calculated a-coefficient, it implies that the result is statistically significant at the 75 % level, and if $P < 0{,}05$, it is statistically significant at the 95 % level. So, the a-coefficient is correct with a 75 % certainty, resp 95 % certainty (Statistikhjälpen, n.d.). The *P*-value includes the quantity of the dataset compared to the R^2-value, which only describes the relation. Consequently, the more existing data, the greater the statistical significance. That is why the *P*-value will be the main subject of the discussion.

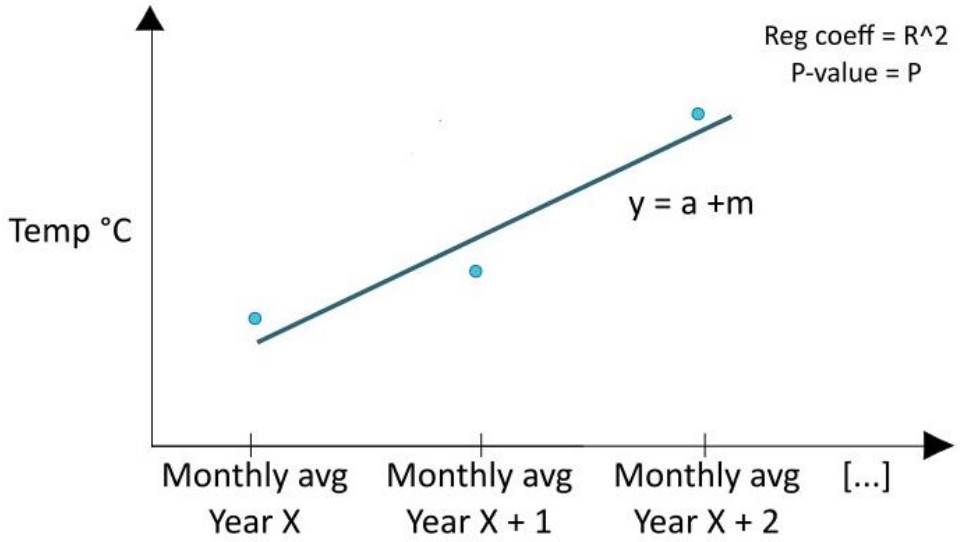

Figure 50. Illustration of "linear regression". A monthly average is calculated for each year, and a linear line is adjusted on top. The a-coefficient describes the slope of the line and represent the change over time.

By comparing these *a*-coefficients for the different stations, it is possible to investigate if similar temperature trends can be found for the eastern Spitsbergen as was seen on Franz Joseph Land.

Franz Joseph Land calculated a value for ΔT that describes the mean temperature change from 2000-2017. It is calculated from the "straight line equation" and the yearly *a*-coefficient from the linear regression analysis, see Equation 3. This temperature change will be calculated the available datasets as well.

$$\Delta T = a * (Year_{last} - Year_{first}) \quad \text{(Eq. 3)}$$

A major problem with this study is that the available datasets from eastern Spitsbergen are so short that it might be difficult to draw any statistically significant conclusions. Data from Longyearbyen will be used to give an overall picture of the general difference between Franz Joseph Land and Svalbard. This station is located more to the west than the others but has

temperature data as far back as 1975 (Nordli et al., 2020 & Fröland et al., 2011). This opens the opportunity to analyze a longer temperature trend from mainland Svalbard compared to Franz Joseph Land. A linear regression between Franz Joseph Land and Longyearbyen will be calculated for the period of 2000-2017.

5.4 Seasons

Since Arctic regions have a generally colder climate compared to the global average, their meteorological seasons do not follow the calendrical seasons. According to Ivanov et al. (2019), a season is defined as a period when the value of the long-term surface air temperature variability remains constant. The year is because of this divided into season according to Table 3. Summer and winter are the longest seasons, with 4 and 6 months each. Meanwhile, spring and autumn are only one month each. The same grouping of the seasons will be used for this study.

Similar linear regression was calculated for the seasons to evaluate at what season of the year the most notable change occurs.

Table 3. Division of seasons and months.

Winter				**Spring**	**Summer**				**Autumn**	**Winter**	
Jan	Feb	Mar	Apr	May	Jun	Jul	Aug	Sep	Oct	Nov	Dec

5.5 Lapse rate and other parameters

The local variability from eastern Spitsbergen will be investigated. Each parameter for every station from Table 2 will be plotted to visualize the trends over time. Eastern Spitsbergen has a total of six different stations, but all at different altitudes. To take the altitude into account, the lapse rate will be calculated. It is typically measured by sending up a balloon, but this kind of data is unavailable. Instead, the daily lapse rate, which is defined as the vertical temperature change, will be calculated according to Equation 4:

$$\Gamma = -\frac{dT}{dz} \approx -\frac{\Delta T}{\Delta z} = -\frac{T_{\text{Lomonosovfonna 1200}} - T_{other\ station}}{z_{\text{Lomonosovfonna 1200}} - z_{other\ station}} \qquad \text{(Eq. 4)}$$

Each station will be compared to Lomonosovfonna 1200, positioned at the highest altitude. This generates the largest Δz and ΔT possible for most stations. It is important to mention that this is a very simplified calculation assuming only vertical temperature changes and neglects horizontal variations or other external influences.

5.6 Correlation of parameters in between the stations

A scatterplot and its corresponding correlation coefficient will be used to understand what meteorological parameter affects each station's temperature change. A scatterplot can present the relationship between two variables in a dataset, and the correlation coefficient describes this relationship. 1 means a perfect correlation, 0 means no correlation, and -1 means a perfect anti-correlation (Moore et al., 2013).

This analysis will be performed station-wise, where all meteorological parameters for each station will be calculated against that station's temperature. Wind speed against temperature, relative humidity against temperature, surface air pressure against temperature, short wave incoming and outgoing radiation against temperature, and long wave incoming and outgoing radiation against temperature.

6. Results

6.1 Addition of a Gaussian filter

A Gaussian filter was added to the plots to simplify the visualization of how the parameters changed over time. Figure 11 shows an example of how the temperature data from Svenbreen during 2015 smoothed with an applied Gaussian filter with a σ-value equal to 5 days. The Gaussian filter generates a reliable trend and identifies the changes over time. It is essential to remember that the smoothed trend dampens the real min- and max-values.

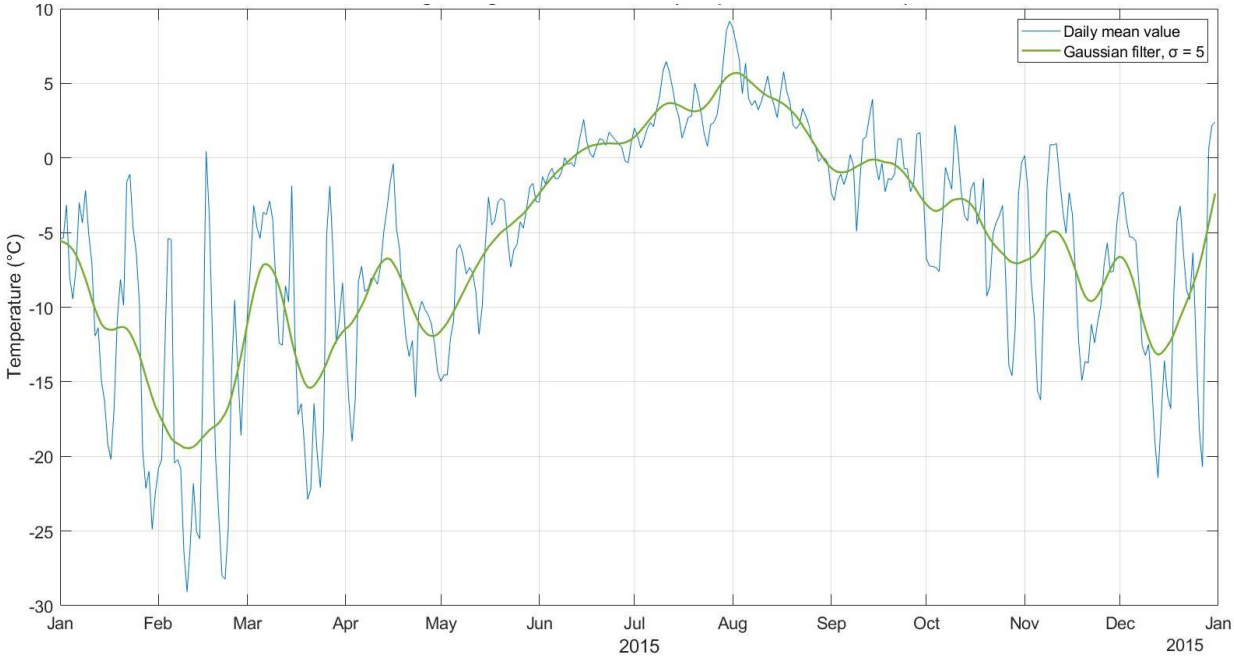

Figure 11. An example of how the temperature data from Svenbreen during 2015 is smoothed out with an applied Gaussian filter with a σ-value equal to 5.

6.2 Temperature plots over time

When plotting measured temperature over time (Figure 12) it is possible to get an overall visual image of the temperature progression for each station from eastern Spitsbergen. These meteorological setups are relatively new, with the oldest one only having data logged from 2009.

Generally, it can be observed that the temperature is related to the site's altitude, where higher altitude gives lower measured temperatures. Even with an applied Gaussian filter, the winter's temperature fluctuates more and remains more stable during the summer. For example, Pyramiden shows maximum summer temperature between the range of 7 – 10 °C; meanwhile, Lomonosovfonna 1200 shows minimum winter temperature between the -17 – -30 °C. Once again, these min- and mix-values are not the actual measured temperatures, but this result indicates a stronger variation in temperature in winter.

This figure also marks the notable spring that occurred in 2017. Temperatures near the sea level were as low as the temperatures at the elevation of 1200 m.a.s.l. Another remarkable event was in the late winter/spring of 2020, where the stations with available data showed temperatures lower than -20 degrees, which had not happened in previous years.

However, it is impossible to see any noticeable year-on-year increases/decreases in temperature in Figure 12 for any stations. This will be studied in section 6.3.

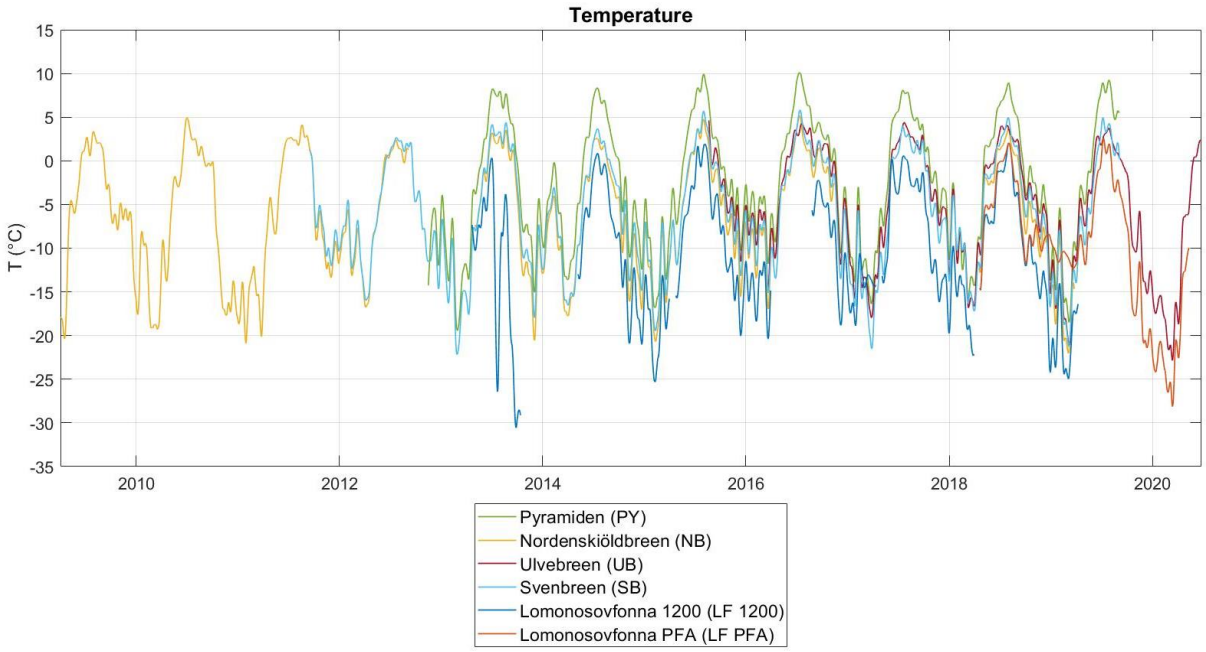

Figure 12. Temperature data over time for all eastern Spitsbergen stations, with an applied Gaussian filter.

6.3 Comparison of temperatures with linear regression

Regarding the yearly temperature change, linear regressions have been used. The following tables (Table 4-6) demonstrate each station's calculated linearity *a*-coefficient and its accompanying R^2 and *P*-values. The tables are color-coded according to the extent of the *a*-coefficients and their statistical significance (*P*-value). Negative *a*-values are presented in blue and positive *a*-values are in red for the *a*-coefficient column. A coefficient above 0.5 and below -0.5 is considered extra warm/cold and marked with a shaded color. For the *P*-column, the values are dark green if the *a*-coefficients have a statistical significance of $P < 0.05$, light green if the value has a statistical significance of $P < 0.25$, and grey if the *a*-coefficient is insignificant. As mentioned, the *P*-value will be considered more compelling than the R^2-value since the *P*-value takes in quantity, which is why the R^2-column remains white and left without discussion.

It is possible to compare the result from eastern Spitsbergen against the results from Franz Joseph Land using this table. As expected, low statistical significance was observed for the linear coefficients for the stations in eastern Spitsbergen. This is due to the short data series. Therefore, only the three longest available series will be presented. For all other stations, their results can be found in appendix A.3.1 and A.3.2.

Table 4 present the results for Nordenskiöldbreen, Svenbreen, and Pyramiden versus Franz Joseph Land with an available period of 2009 – 2017, 2011 – 2017, and 2012 – 2017 respectively. It is difficult to draw any scientifically valid conclusions as only a few values demonstrate statistical significance. Values from Franz Joseph Land have a particular low

significance, with only one reliable value for each observation. The discussion of this data would be speculative. But to leave this data without a comment would on the other hand be a loss to neglect to show the rare data existing in this area.

Table 4 shows that the temperature trends do not tend to follow each other. The worst comparison is between Franz Joseph Land and Pyramiden (2012-2017), where Franz Joseph Land only has four months of warming. For Pyramiden, it is the opposite, with only three months of cooling. Svenbreen and Franz Joseph Land (2011-2017) have the same pattern, but Franz Joseph Land appear to be delayed. Svenbreen gets warming in the late autumn/early winter. Meanwhile, Franz Joseph Land gets warming during mid-winter/late winter. The best comparison suits between Nordenskiöldbreen and Franz Joseph Land (2009-2017), where the winter from January to April is exposed chiefly for heating.

Table 4. Monthly linear regression coefficients for Franz Joseph Land compared to Nordenskiöldbreen, Svenbreen and Pyramiden, and its corresponding statistical significance.

Month	2009-2017						2011-2017						2012-2017					
	Franz Joseph Land (FJL)			Nordenskiöldbreen (NB)			Franz Joseph Land (FJL)			Svenbreen (SB)			Franz Joseph Land (FJL)			Pyramiden (PY)		
	a (ºC/yr)	*R^2*	*P <*	*a (ºC/yr)*	*R^2*	*P <*	*a (ºC/yr)*	*R^2*	*P <*	*a (ºC/yr)*	*R^2*	*P <*	*a (ºC/yr)*	*R^2*	*P <*	*a (ºC/yr)*	*R^2*	*P <*
Jan	0,627	0,13	0,33	0,832	0,27	0,29	0,579	0,06	0,60	-0,910	0,32	0,25	0,029	0,00	0,98	-0,438	0,06	0,69
Feb	0,705	0,14	0,32	0,173	0,01	0,86	0,293	0,01	0,80	-0,104	0,00	0,94	-0,097	0,00	0,95	0,409	0,02	0,84
Mar	0,632	0,17	0,27	0,633	0,30	0,21	0,211	0,01	0,81	-0,436	0,06	0,65	0,160	0,00	0,90	0,436	0,05	0,73
Apr	0,598	0,18	0,25	0,625	0,12	0,41	-0,079	0,00	0,90	0,315	0,07	0,62	-0,109	0,00	0,91	0,361	0,06	0,69
May	-0,088	0,03	0,67	0,013	0,00	0,97	-0,379	0,39	0,13	-0,244	0,03	0,74	-0,489	0,42	0,16	-0,157	0,01	0,87
Jun	0,170	0,09	0,44	0,015	0,00	0,89	-0,114	0,09	0,52	0,147	0,19	0,39	-0,054	0,01	0,83	0,232	0,38	0,27
Jul	0,035	0,04	0,63	0,114	0,16	0,32	0,029	0,02	0,79	0,202	0,21	0,37	0,003	0,00	0,99	0,046	0,01	0,88
Aug	0,033	0,01	0,77	-0,138	0,14	0,37	-0,139	0,19	0,33	-0,086	0,03	0,73	-0,191	0,22	0,35	-0,182	0,12	0,56
Sep	-0,090	0,06	0,55	-0,104	0,03	0,71	-0,204	0,18	0,35	0,203	0,10	0,48	-0,220	0,14	0,47	0,509	0,39	0,26
Oct	-0,295	0,16	0,32	0,487	0,24	0,27	-0,104	0,01	0,80	0,887	0,54	0,06	-0,106	0,01	0,85	1,582	0,72	0,07
Nov	-0,427	0,05	0,58	0,444	0,07	0,57	0,514	0,05	0,63	0,913	0,52	0,07	0,606	0,04	0,69	1,655	0,79	0,02
Dec	-0,239	0,04	0,62	0,318	0,09	0,51	-0,639	0,18	0,34	0,466	0,40	0,13	-0,017	0,00	0,98	0,804	0,70	0,04

Colder	*0 < a < -0,5*
Much colder	*a < -0,5*
Warmer	*0 > a > 0,5*
Much warmer	*a > 0,5*

Significant 95%	*P < 0,05*
Significant 75%	*0,06 < P < 0,25*
Insignificant	*P > 0,26*

Data from Longyearbyen has been used, because of the low significance of the short data series available for eastern Spitsbergen. It has then been possible to analyze similarities/differences with the results from Franz Joseph Land during the time interval 2000-2017. It is worth mentioning that values for Franz Joseph Land are directly copied from Ivanov et al. report. Although the analysis of data from Longyearbyen will not be feasible to answer the question about the temperature development for eastern Spitsbergen, it gives a result that will be more reliable. Tables 5 and 6 compare Franz Joseph Land and Longyearbyen, both month-by-month and seasonally. At first glance, it is possible to notice that the significance level increases drastically. When looking into the month-by-month comparison (Table 5), one can demonstrate that both trends show a more similar temperature trend compared to Tables 4 with shorter periods. Differences between the two sites are that Franz Joseph Land has two negative coefficients during May, and June (nonetheless not significant), indicating cooling, compared to Longyearbyen with only positive coefficients. Franz Joseph Land also seems to have stronger warming with coefficients greater than 0.5, all with statistical significance of $P < 0.05$. This occurs during February, Mars, and November. Even if Longyearbyen does not have as strong coefficients, the winter month also appear to have greater warming during the winter months, and the most notable change occurs in March with an *a*-coefficient of 0.453 °C/year ($P < 0.01$).

A signal of significant warming for the winter can also be motivated by Table 6, showing the seasonal changes. The most crucial change for both stations occurs in winter, where Franz Joseph Land has a coefficient of 0.284 ($P < 0.10$) and Longyearbyen 0.254 ($P < 0.02$). Summer shows the contrary, which has the smallest increase with coefficients of 0.034 ($P < 0.25$) and 0.072 ($P < 0.01$) respectively.

The result of Ivanov et al.'s (2019) report was that the yearly mean temperature between 2000-2017 raised with 5.20 °C. A similar result was calculated for Longyearbyen, where the mean temperature increased by 5.65 °C.

Table 5. Monthly linear regression coefficients for Franz Joseph Land compared to Longyearbyen, and its corresponding statistical significance.

Month	2000-2017					
	Franz Joseph Land (FJL)			Longyearbyen (LYB)		
	a (ºC/yr)	***R^2***	***P <***	***a (ºC/yr)***	***R^2***	***P <***
Jan	0,448	0,21	0,10	0,314	0,14	0,13
Feb	0,537	0,27	0,05	0,273	0,16	0,10
Mar	0,525	0,34	0,05	0,453	0,33	0,01
Apr	0,393	0,34	0,05	0,095	0,02	0,58
May	-0,012	0,00	0,90	0,082	0,09	0,23
Jun	-0,029	0,05	0,40	0,079	0,28	0,02
Jul	0,014	0,04	0,45	0,043	0,11	0,18
Aug	0,012	0,02	0,65	0,002	0,00	0,97
Sep	0,187	0,37	0,05	0,165	0,36	0,01
Oct	0,313	0,30	0,05	0,171	0,14	0,13
Nov	0,564	0,30	0,05	0,198	0,12	0,17
Dec	0,321	0,14	0,15	0,188	0,09	0,22
Year	0,289	0,50	0,05	0,314	0,14	0,13
ΔT	5,20			5,65		

Table 6. Seasonal linear regression coefficients for Franz Joseph Land compared to Longyearbyen, and its corresponding statistical significance.

Season	2000-2017					
	Franz Joseph Land (FJL)			Longyearbyen (LYB)		
	a (ºC/yr)	***R^2***	***P <***	***a (ºC/yr)***	***R^2***	***P <***
Winter	0,284	0,24	0,10	0,254	0,32	0,02
Spring	0,051	0,03	0,55	0,082	0,09	0,23
Summer	0,034	0,11	0,25	0,072	0,44	0,01
Autumn	0,209	0,13	0,25	0,171	0,14	0,13

To simplify the understanding of these tables, only the statistically significant monthly values are plotted and summarized in Figure 13. It is easier to see that more substantial warming occurs during the winter while the summer is kept more stable. It is also clear that the two stations follow the same temperature pattern month by month. However, the month of November differs, with Franz Joseph Land having a much more significant increase. It is also notable that results from Franz Joseph Land are not as statistically significant as those from Longyearbyen, indication larger variability.

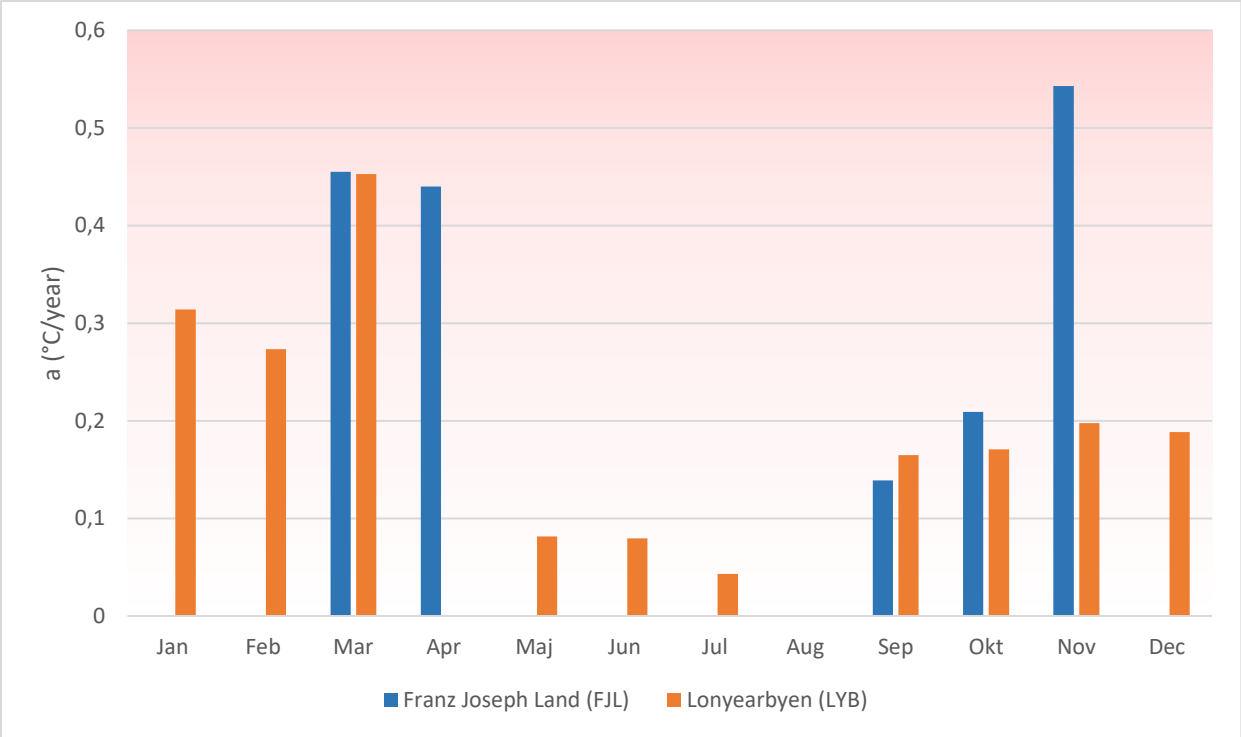

Figure 6. A summary of all statistically significant a-coefficients from Franz Joseph Land and Longyearbyen,

Since it was impossible to compare the temperature changes between eastern Spitsbergen and Franz Joseph Land using regression analysis, Figure 14 has been constructed. It shows how the temperature trend from Franz Joseph Land relates to the rest of the stations. Here, the mean temperature for Franz Joseph Land is generally lower than eastern Spitsbergen's. Franz Joseph Land roughly follows the trend for Lomonosovfonna 1200, which is located at an altitude of 1200 m.a.s.l., compared to Franz Joseph Land, with an altitude of about 20 m.a.s.l.

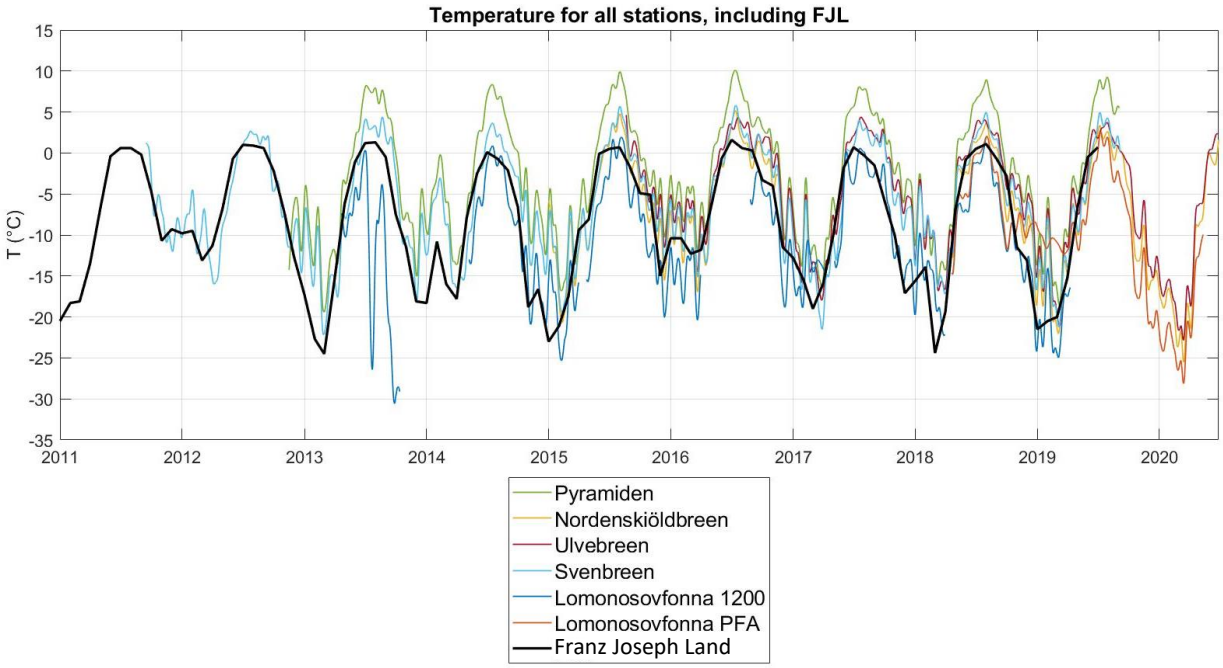

Figure 14. Temperatures over time for all stations, including Franz Joseph Land (black), with an applied Gaussian filter.

6.4 Other parameters

Other meteorological parameters have also been examined, such as surface air pressure, relative humidity, wind speed, short- and long-wave incoming, and outgoing radiation, to understand each station's local climate. It is mentioned in Table 2 which stations have which type of data logged. When plotting these parameters over time, only wind speed and relative humidity revealed some noteworthy results and are the only figures that will be presented. Trends for the other parameters either lacked much data making comparison difficult or were following the expected pattern, such as the highest surface air pressure at the lowest located station. Therefore, those plots will not be presented in the result but can be found in Appendix A.2.

Figure 15 shows that the measured wind speed differs depending on the station's location. The black line indicates the average wind speed for all stations. Ulvebreen, as well as Nordenskiöldbreen, measures windspeeds way above the average. These trends are plotted using a Gaussian filter, which damped the real min- and max values. Nevertheless, 2016 shows winds speed for Ulvebreen and Nordenskiöldbreen up to 9 m/s, compared to the average of 6 m/s. For Pyramiden and Svenbreen, the wind speeds are lower, where the maximum speed in the graph does not exceed 5 m/s. The figure also shows a seasonal cycle where all stations have stronger wind speeds during winter than summer.

Figure 16 shows that the relative humidity at Pyramiden differs drastically from the rest of the stations and with values way lower than average, demonstrating considerably drier air. According to the graph, the lowest measured humidity reaches 60% in late winter/spring. The relative humidity is kept within a range of about 75 – 95% for the other stations. The maximum relative humidity is found at Lomonosovfonna 1200, where concentrations go above 95%.

There is also an apparent seasonal variation, with rising relative humidity in summer and sinking in winter, i.e., the winter has a drier climate.

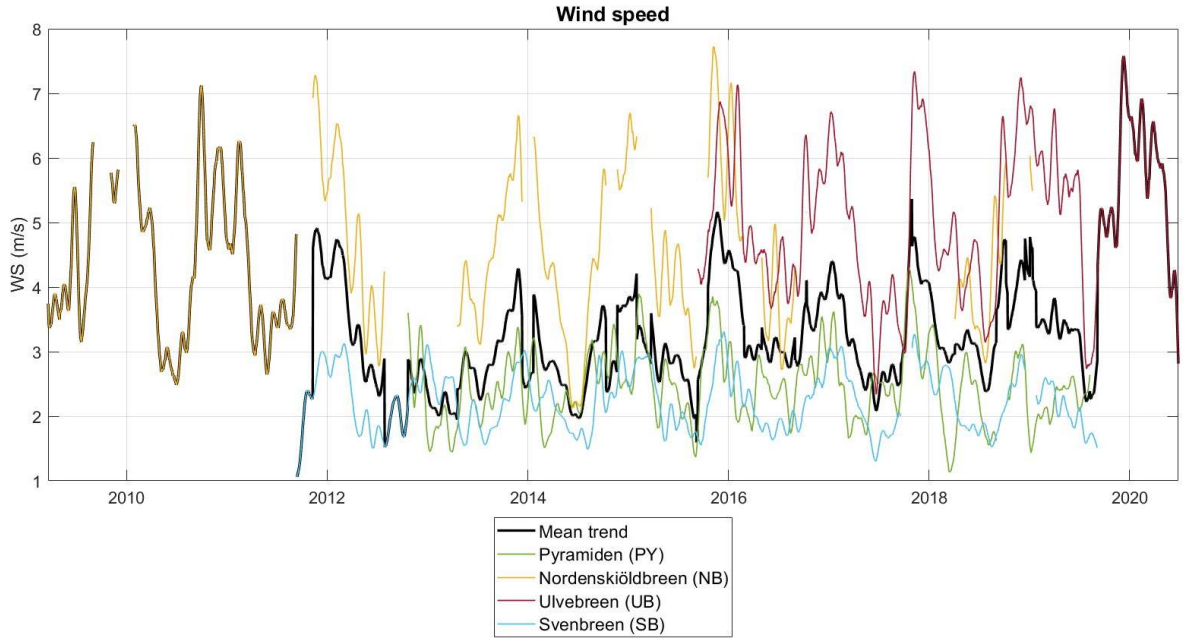

Figure 15. Measured wind speed for all stations, with an applied Gaussian filter. The black trend is the mean trend.

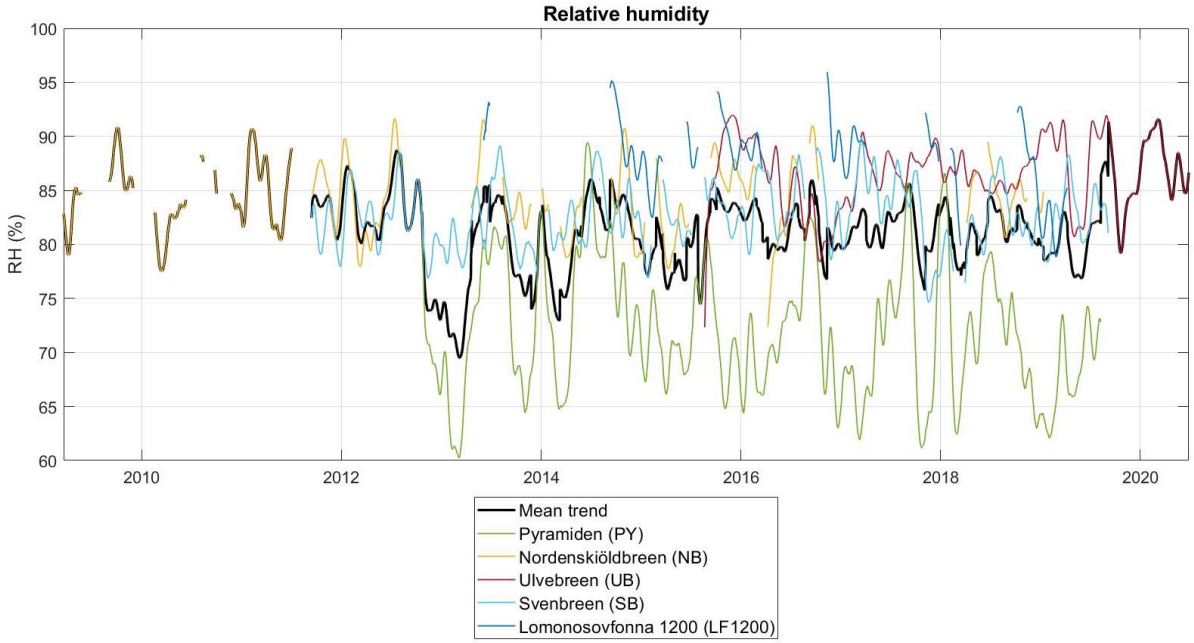

Figure 16. Measured relative humidity for all stations, with an applied Gaussian filter. The black trend is the mean trend.

6.5 Lapse rate

The lapse rate has been calculated by comparing the temperatures for each station against the highest located station, Lomonosovfonna 1200, to minimize the uncertainty in the results. However, this means that the result for Lomonosovfonna PFA, also situated at an altitude of 1144 m.a.s.l, will have unreliable results because *dz* in Equation 4 will be too small (only 56m). In addition to outliers from Lomonosovfonna PFA, the lapse rate in 2013 showed values up to 25 °C/km, indicating an error. To enable a visual analysis of the lapse rate, values from Lomonosovfonna PFA and the year 2013 have been excluded from the results (Figure 17), and the trend with these included can be found in Appendix A.1.1.

Figure 17 shows that the lapse rate differs depending on the vertical positioning of the station. Pyramiden with the lowest altitude corresponds to a higher lapse rate. Nordenskiöldbreen, Ulvebreen, and Svenbreen are located at higher altitudes and have all lower values but roughly follow the same pattern. The lapse rate values range from 3 to 9 °C/km, with a rising lapse rate in winter and a falling lapse rate in summer. Another outlier is the dip that occurred in March 2017. The lapse rate goes down to a negative value, towards a minimum of -7 °C/km.

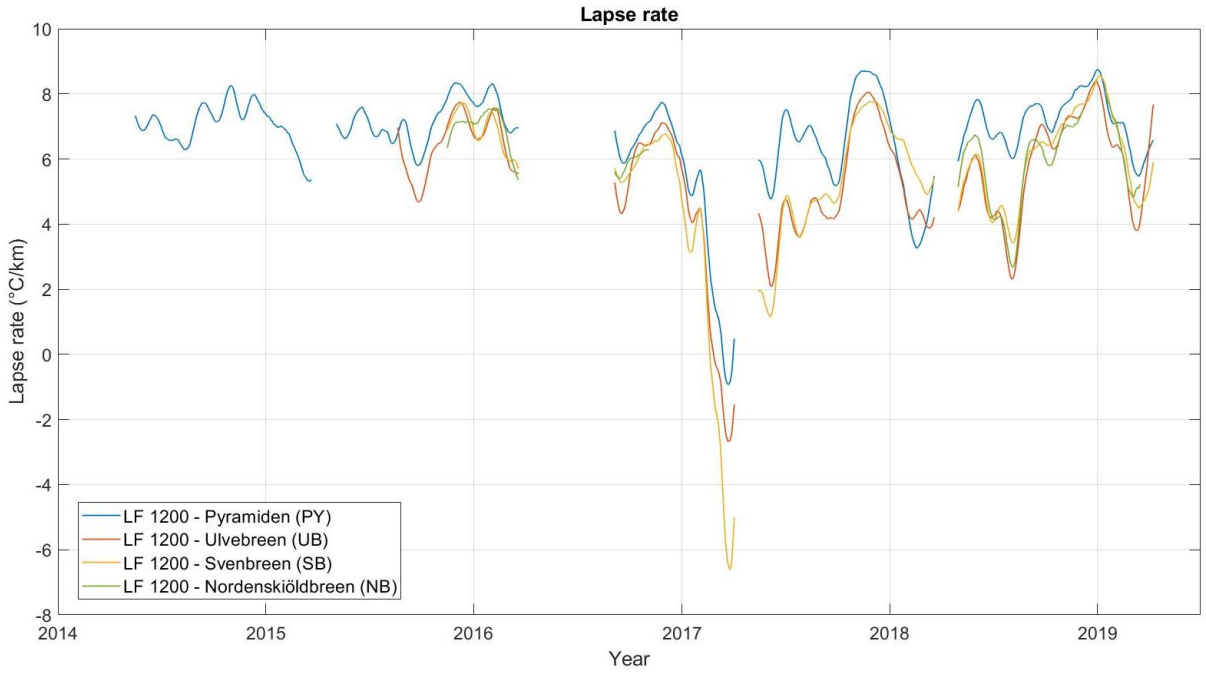

Figure 17. The calculated lapse rate related the highest one Lomonosovfonna 1200. The trends have an applied Gaussian filter.

6.6 Correlation of parameters

Although the different parameters seem to vary between the stations, it is not apparent what influences the temperature changes. To explain this, a scatterplot and its corresponding correlation coefficient have been presented. The calculations are performed station-wise, where all parameters for the specific station (see Table 2) have been compared against that station's temperature. It is impossible to determine which parameter is driving temperature changes for Lomonosovfonna PFA as it has only logged the temperature and are therefore not presented in

the graph. Figure 18 demonstrates the correlation coefficient, and the scatterplots can be found in Appendix A.4.

It is seen that the temperature at Ulvebreen and Nordenskiöldbreen is strongly correlated to the incoming and outgoing longwave radiation, with coefficients almost up to 1, indicating that the longwave radiation is related to the surface temperature. Lomonosovfonna 1200 also has measured values for the radiation but does not show an equally strong correlation. The most vital parameter for that station is relative humidity. Neither Pyramiden nor Svenbreen has an apparent parameter correlating to the temperature, since the values are too low. The strongest for Pyramiden is the relative humidity, and for Svenbreen, it is the incoming short-wave radiation and wind speed.

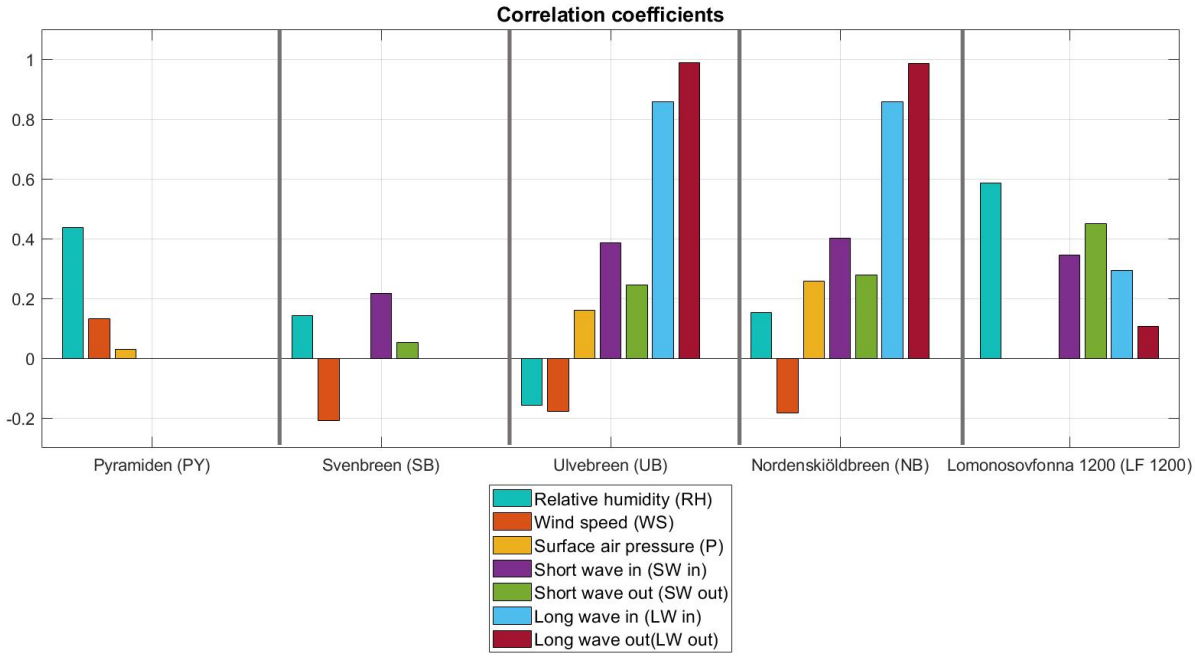

Figure 18. Calculated correlations coefficients between each parameter related the temperature, station-wise. All stations do not have measurements for all parameters, why some stations have fewer number of bars. Lomonosovfonna PFA is not presented in the figure since it has only measured temperature.

7. Discussion

7.1 Temperature changes in eastern Spitsbergen compared to Franz Joseph Land.

This report cannot support a conclusion that the temperature of the eastern Spitsbergen has increased comparably to the Franz Joseph Land. The same method as the Franz Joseph Land, linear regression, had to be used to draw this conclusion. It was impossible to make an arbitrary comparison between Franz Joseph Land and the six stations as the results did not show statistical significance. However, it is possible to conclude that the temperature for Longyearbyen, southwest of the actual area of this report, shows similar temperature trends since the station has measurement data further back in time.

When the report from Ivanov was published in 2019, scientists were surprised by the remarkable temperature increase of 5.2 °C from 2000-2017 for Franz Joseph Land. Though, this high value has also been calculated for Longyearbyen, with a rise of 5.65 °C during the same period. Whether this result can be generalized for the whole Svalbard or whether it is only local to Longyearbyen is something that should be investigated further. Longyearbyen is the community where most of Svalbard's population lives, and the temperature may be affected by a local heat island. In addition, Longyearbyen is located in the center of Svalbard, and more to the west than the remaining six stations on which this study is based. The southwest of Svalbard would likely have weaker trends, while the northeast would likely have experienced stronger temperature trends. This is related to changing sea ice conditions which have a larger impact in the northeast of Svalbard, which usually is surrounded by sea ice in winter and spring, but the extent is now reducing. In the southwest, there is never any sea ice. The presence of sea ice tends to give lower temperatures as it cools the surface. The extremely cold temperature minima in winter occur when the wind blows from the cold sea ice onto Svalbard.

But, by observing the temperature trends, it possible to discuss how the station´s temperatures are related. Figure 19 only presents the temperatures for Pyramiden (the warmest), Lomonosovfonna 1200 (the coldest), and the external stations Franz Joseph Land and Longyearbyen. What can be seen is two strong relations. Firstly, the trend from Franz Joseph Land follows the one for Lomonosovfonna 1200, meaning that temperatures at an altitude of 1200 m.a.s.l correspond to the temperatures on a higher latitude with around two decimal degrees. Secondly, the other strong relation is Longyearbyen and Pyramiden. Their temperatures seem to follow each other well. They are positioned close to Isfjorden, so it makes sense that they have similar trends as the water surface will interact with the atmosphere and impact the properties of the air in the area. This makes it possible to assume that the temperature increase seen on Longyearbyen can also be made for Pyramiden.

Since it was possible to see that external temperature series correlated to the warmest and the coldest from eastern Spitsbergen, one can speculate that climate warming has occurred all over the area.

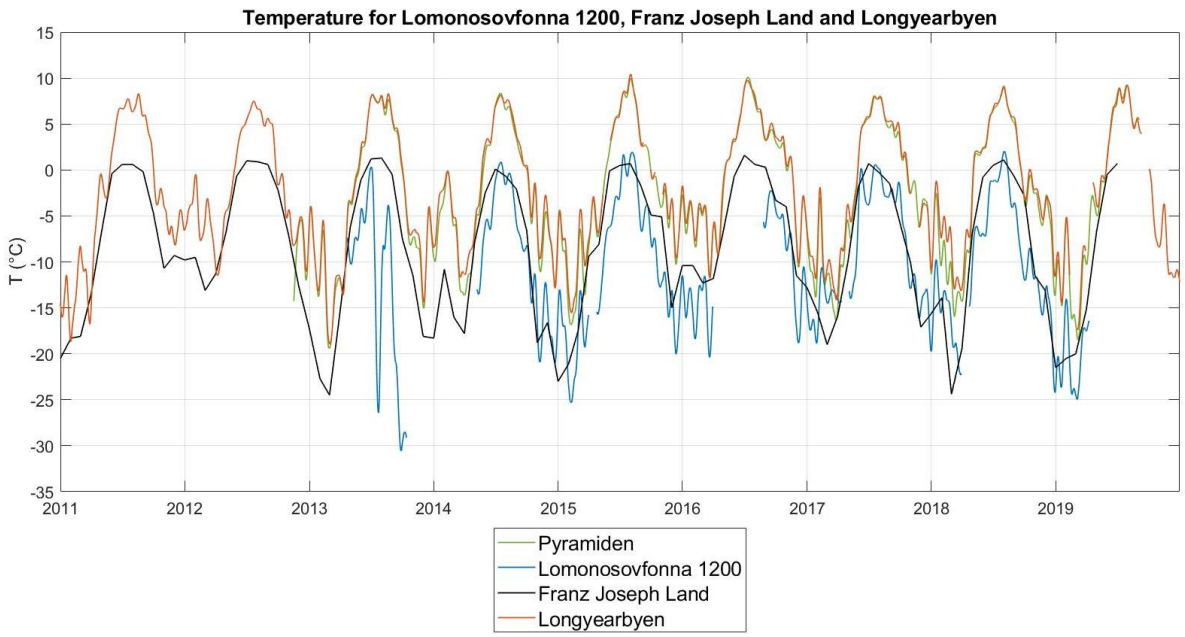

Figure 19. Temperatures over time for Pyramiden (the warmest), Lomonosovfonna 1200 (the coldest), and the external stations Franz Joseph Land and Longyearbyen, with an applied Gaussian filter.

It is essential to recall that the trends have an applied Gaussian filter that dampens fluctuations, which explains why no extreme temperatures can be seen. It is also clear that Lomonosovfonna 1200 has reasonably warmer temperatures than expected at an altitude of 1200 m.a.s.l. and is located on a snow-covered glacier. This is mainly because the climate at these altitudes is so severe that the weather station is often ice-covered. When the instruments are covered with snow and ice, the real values are subdued. The station then measures the surface temperature rather than the air temperature, which is not necessarily the same. The surface temperature depends on all energy fluxes at the surface and is strongly related to air temperature, but there are other factors, like cloud cover, humidity, etc., that also affect surface temperature. The data series from this station also has many gaps in its data; see Figure 20 for what the station can look like during a cold day.

Figure 20. Sergey Marchenko works on the entire snow- and ice-covered measurement station Lomonosovfonna 1200 (Veijo Pohjola, 2022).

7.2 Local variability for stations on eastern Spitsbergen

The analysis of each parameter was done to gain an understanding of the temperature variance between the stations. The trends that gave interesting results were mainly wind speed and relative humidity. Figure 15 showed a significant difference in wind speed where both Nordenskiöldbreen and Ulvebreen had more than twice the measured speeds compared to Pyramiden and Svenbreen. Ulvebreen, located along the eastern coast, seems strongly influenced by the cold and strong northeasterly winds that move across the archipelago. Nordenskiöldbreen also shows high wind speeds, mainly because of its higher altitude and position in a valley. Wind tunnels are usually created along the valley because air gets pressed and forced along the valley itself. Pyramiden and Svenbreen have lover wind speeds because the stations are sheltered by the large surrounding mountain massifs, which protect them from the strong and cold winds. Still, this does not really help to explain temperature variability, which depends more on large-scale wind direction. If winds during a winter would blow more frequently from the southwest, where there is no sea-ice, the temperature in Svalbard would be relatively warmer than if the dominant wind direction would be from the northeast.

Figure 16 also exhibited surprising results. Pyramiden, located closest to Isfjorden and at the lowest altitude, appears to be the station with the lowest relative humidity. At first glance, this seems questionable because one would expect Isfjorden to contribute to a humid climate. Nevertheless, this station seems to have the most substantial yearly amplitudes, indicating much dryer winters than summers. This strong variability can be connected to the ice-covered Isfjorden during winter, leading to a local dryer climate. Compared to the other stations, the much dryer winters may imply that other factors impact this station.

The altitude influences the local temperature, and Figure 12 shows that the higher the station's altitude, the colder the temperatures. Therefore, the lapse rate was calculated and analyzed mainly to investigate how vertical stratification varies in time and space. First and foremost, it is essential to recall that this calculation is a simplification where factors that usually are included have been neglected. Among other things, Equation 4 is calculated by comparing all stations against Lomonosovfonna 1200, the station at the highest altitude. This means that the higher the stations are located, the smaller the height difference (Δz) in the equation, which increases the uncertainties of the result. An example is how the lapse rate trend for Lomonosovfonna PFA had to be excluded from the analysis as the results were too poor (see appendix A.1.1). The temperature trend for Lomonosovfonna 1200 also consists of many data gaps for the reasons mentioned above, which further degrades the credibility of the calculated lapse rate. The results must therefore be analyzed carefully.

Figure 17 shows that winters indicate higher lapse rates compared to summers. The figure also shows that Pyramiden generally has higher lapse rate values than the remaining stations. In addition, the graph shows a significant dip during March 2017 with a negative lapse rate. Either there was a strong inversion, a generally cold spring, or a large instrumental error. Figure 12 shows that the lower stations' temperature was significantly colder than in other years, except for Lomonosovfonna 1200. Since the lapse rate is calculated as the quotient of the temperature difference (ΔT) by height difference (Δz), the lapse rate values become much smaller if ΔT is

reduced as much as they did in March 2017. Additionally, the temperatures for Lomonosovfonna 1200 may have been dampened due to icing.

The differences in the lapse rate values between the seasons may be linked to the katabatic winds that occur in mountainous areas and the creation of inversions. At the top of the mountains, cold air is produced. Due to gravity, the air masses flow down the mountainsides into the valley. These cold and dry air masses accumulate at the bottom of the valley, which generates settles like a cap and captures outgoing heat from the ground. This creates an inversion so that the temperature rises with altitude. In winter, this is more prevalent partly because there is a greater production of cold air on top of the mountain and that warm and moist air from the Atlantic is coming in over Svalbard. The temperature gradient can be up to 10 °C, creating inversions at even higher altitudes. This leads to warmer surface temperatures and hence higher values of lapse rate. Under section 3.4.3, it was mentioned that the most vital amplified feedback in the Arctic is the lapse rate feedback; thus, the surface warming intensifies. Figure 17 indicates that this occurs effectively during the winter and can describe one reason for why the winters are extra vulnerable to Arctic warming, as seen in both Figure 12 and Table 6. It is essential to mention that Table 6 seems to have an error for Franz Joseph Land. The values are, as mentioned, straight copied from their report. Since the seasons were divided as in Table 3, where autumn is defined as only October, one would expect the “October value” to be equal to the “winter value” in Tables 5 and 6. This is not the case, indicating some errors. Even if there might be other errors in this table, it does not change the conclusion that winter tends to show the strongest warming.

To create these inversions, a stable atmosphere is required. However, Svalbard is considerably milder, wetter, and cloudier than the average for this latitude (Hanssen-Bauer et al., 2019) which often generates turbulent weather conditions and an unstable atmosphere, and thus no "lid" that captures warm air. Pyramiden is reasonably leeward of surrounding mountains, which may facilitate stable conditions in contrast to the other stations. Therefore, the warm air can be "closed in" by heavier cold and dry air masses from above, resulting in enhanced warming and explaining why Pyramiden has the largest lapse rate values. This can also be linked to why Pyramiden has the driest air (Figure 16): cold air masses glide down the mountainsides into the valley. Pyramiden is additionally located without getting affected by the surrounding stronger winds. This can also be confirmed by the surface air pressure (appendix A.2.5), where Pyramiden shows the highest pressure of all stations.

7.3 Correlation of parameters

Figure 18 revealed that temperature correlated almost 100% with incoming and outgoing longwave radiation. It makes sense since, according to theory, the temperature is strongly linked to the radiation balance. Usually, the incoming shortwave radiation has the strongest correlation to the temperature. Since Svalbard is located above the Arctic circle, half of the year there is no incoming shortwave radiation. Instead, Svalbard’s temperature is constantly affected by the long wave radiation. Emitted long wave cools down the surface, meanwhile, reflected longwave radiation to the surface increases the temperature all year around. However, Lomonosovfonna 1200 did not show the same trend. This is because the measurements from this station have

been very disturbed by external influences, mostly icing, especially for the in- and outgoing radiation, see Appendix A.2.1-A.2.4.

Since wind speed and relative humidity stood out under section 6.4, their scatterplots are presented below. Although the correlation is not very strong, it is possible to see a relationship between the parameters. Figure 21 shows that colder temperatures for Svenbreen, Nordenskiöldbreen, and Ulvebreen occur with stronger winds. For Pyramiden, it is the opposite, where more wind means warmer temperatures. This may also be linked to what has been discussed earlier, that Pyramiden is in the lee of the strong and colder northeasterly winds. The temperature is affected by the warmer winds coming in from Isfjorden. This might be another reason for why Pyramiden is generally warmer than the rest of the stations. Another explanation could be that Svenbreen, Ulvebreen, and Nordenskiöldbreen are all on glaciers and katabatic effects are stronger in winter when it is colder.

In relative humidity, Figure 22, it can be pointed out that Ulvebreen is the only one with a negative trend, meaning the more humid the air, the colder the temperatures. This strengthens the argument that Ulvebreen is vulnerable to cooling by Northerly advection due to its positioning near the Barents Sea.

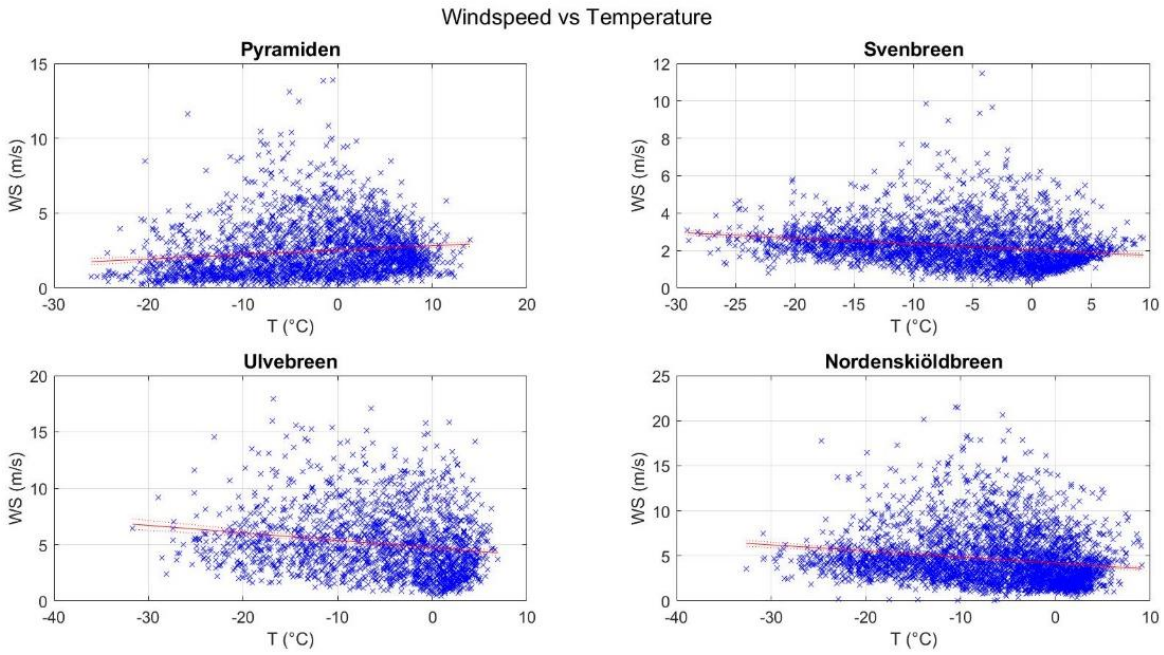

Figure 21. Scatterplots between windspeed and temperature for Pyramiden, Svenbreen, Ulvebreen and Nordenskiöldbreen.

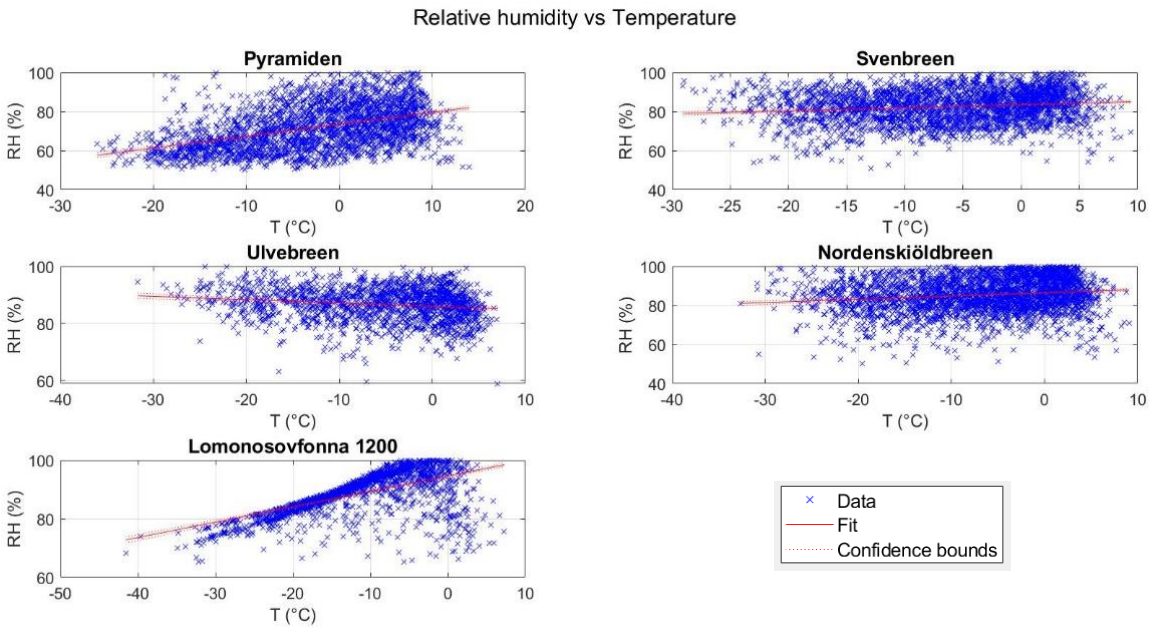

Figure 22. Scatterplots between relative humidity and temperature for Pyramiden, Svenbreen, Ulvebreen, Nordenskiöldbreen and Lomonosovfonna 1200.

7.4 Final remarks

These results suggest that the positioning of each station has a strong influence on its local climates, such as its altitude, proximity to the open sea, the influence of winds, shading, cloud cover. This implies that it is important to consider the stations' locations when analyzing temperature data. Local climate and external factors play a role in large-scale temperature changes. This means that the presumption from Ivanov's report should be questioned where they combined two shorter series into one longer one with the explanation that the climates are considered equal. This is despite the stations being about 100km apart, and the open ocean surrounds one station while the other is surrounded by ice-covered water. However, this does not affect the results in this report as only the period of interest was 2000-2017 from one station. Thus, their long-term results may be doubted. In addition, this method of doing linear regression to analyze climate change, has been criticized as a reliable method by researchers. They argue that "such changes do not necessarily occur linearly" (Hanssen-Bauer et al., 2019).

Although the results are based on several uncertainties, it is still clear that the warming of Svalbard is occurring, which could bring further consequences in the future. The Arctic is particularly vulnerable to climate change due to Arctic climate feedback that accelerates the process. Among other things, calculations have shown that by 2050 the Barents Sea is expected to be ice-free all year round (Smedsrud et al., 2013). The heat exchange between the surface and the surrounding atmosphere grows with an open ocean and intensifies warming. As mentioned, the Barents Sea acts as a heat exchanger for the rest of the global oceans, where warm water is cooled, and degradation of this process can have large-scale effects. However, more research is required to predict the future and, above all, longer data series to understand the long-term changes.

8. Conclusions

- The rate of warming of Longyearbyen is comparable to the warming found for Franz Joseph Land. It can be speculated that similar trends occur across the entire archipelago. This, because the temperatures of Pyramiden tend to follow the Longyearbyen record, and that Lomonosovfonna 1200 follow the Franz Joseph Lands record.
- Winters are most vulnerable to arctic warming.
- The local warming for eastern Spitsbergen cannot be confirmed because the available data series are too short to draw significant conclusions.
- The temperature and climate vary between the stations. When analyzing climate change, it is essential to consider local topography.
- Incoming and outgoing radiation are the main drivers of temperature change. Wind speed and relative humidity do not have equally strong correlation to temperature, but a relation can be seen.

References

Boeke, R., Taylor, P., Sejas, S. (2020). *On the Nature of the Arctic's Positive Lapse-Rate Feedback.* Retrieved March 30, 2022, from https://doi.org/10.1029/2020GL091109

Brett, M (2016). *An introduction to smoothing.* Retrieved September 14, 2022, from https://matthew-brett.github.io/teaching/smoothing_intro.html

Britannica (2022). *Svalbard.* Retrieved March 22, 2022, from https://www.britannica.com/place/Svalbard

Cronin, T. W. (2020). *How well do we understand the Planck feedback?* Retrieved March 30, 2022, from https://web.mit.edu/~twcronin/www/document/Cronin2020_PlanckQJ.pdf

Hanssen-Bauer, E.J. Førland, H. Hisdal, S. Mayer, A.B Sandø, A. Sorteberg (2019). *The climate in Svalbard 2100 – s knowledge base for climate adaptation.* Retrieved April 26, 2022: https://www.miljodirektoratet.no/globalassets/publikasjoner/M1242/M1242.pdf

Hemond, H. F., & Fechner, E. J. (2015). *The Atmosphere. Chemical Fate and Transport in the Environment, 311–454.* Retrieved September 01, 2022: https://doi.org/10.1016/B978-0-12-398256-8.00004-9

Jaadi, Z (2021). *A Step-by-Step Explanation of Principal Component Analysis (PCA) | Built-In.* Retrieved June 3, 2022, from https://builtin.com/data-science/step-step-explanation-principal-component-analysis

Laurin, S., Sören Färnlöf, S., Birgitta Löfstedt, M., Birgitta Löfstedt, S., & och Gun-Britt Rosen Lars-Göran Nilsson, S. (1994). *METEOROLOGI-ett häfte om väder och klimat från SMHI.* Retrieved April 26, 2022: *https://www.smhi.se/polopoly_fs/1.165429!/Meteorologi_ett_hafte-om_vader_och_klimat.pdf*

Marchenko, S., V.A. Pohjola, R. Pettersson, W.J.J. van Pelt, C.P. Vega, H. Machguth, C.E. Bøggild and E. Isaksson (2016). A plot-scale study of firn stratigraphy at Lomonosovfonna, Svalbard, using ice cores, borehole video and GPR surveys in 2012-2014. *Journal of Glaciology*, 63, 237, 67-78. doi:10.1017/jog.2016.118

Marchenko, S., W.J.J. van Pelt, B. Claremar, H. Machguth, C.H. Reijmer, R. Pettersson and V.A. Pohjola (2017). Parameterizing deep water percolation improves subsurface temperature simulations by a multilayer firn model. *Frontiers in Earth Science: Cryospheric Sciences*, 5, 16. doi:10.3389/feart.2017.00016

Moore, D. S., Notz, W. I, & Flinger, M. A. (2013). The basic practice of statistics (6th ed.). New York, NY: W. H. Freeman and Company. https://www.westga.edu/academics/research/vrc/assets/docs/scatterplots_and_correlation_notes.pdf

National Geographic Society (2013). *Franz Josef Land.* Retrieved April 26, 2022, from https://www.nationalgeographic.org/projects/pristine-seas/expeditions/franz-josef-land/

Nationalencyklopedin (n.d.). *Svalbard*. Retrieved March 22, 2022, from https://www-ne-se.ezproxy.its.uu.se/uppslagsverk/encyklopedi/l%C3%A5ng/svalbard

Nordli Ö., Wyszyński P., Gjelten H., Isaksen K., Łupikasza E., Niedźwiedź T., Przybylak R (2020). *Revisiting the extended Svalbard Airport monthly temperature series, and the compiled corresponding daily series 1898–2018.* Retrieved 20 October 2022, from https://polarresearch.net/index.php/polar/article/view/3614/11069

Förland E., Benestad R., Hanssen-Bauer I., Haugen J.E., Engen T, (2011). *Temperature and Precipitation Development at Svalbard 1900–2100*. Retrieved 4 November 2022, from http://dx.doi.org/10.1155/2011/893790

Norska Polarinstitutet. (n.d.). *Svalbard*. Retrieved March 30, 2022, from https://web.archive.org/web/20090503130222/http://npweb.npolar.no/geografi/svalbard

P. Pandit, (2021). *Arctic amplification. Extreme Arctic weather: problems for wildlife and people*. Retrieved March 22, 2022, from: https://storymaps.arcgis.com/stories/944e1621359a467983d7d0bc3e619d6b

Previd M., Smith K., Polvani L. (2021). *Arctic amplification of climate change: a review of underlying mechanisms.* Retrieved October 20, 2022, from: https://iopscience.iop.org/article/10.1088/1748-9326/ac1c29/meta

Rantanen, M., Yu Karpechko, A., Lipponen, A., Nordling, K., Hyvärinen, O., Ruosteenoja, K., Vihma, T., & Laaksonen, A. (2022). *The Arctic has warmed nearly four times faster than the globe since 1979*. Retrieved September 19, 2022, from https://doi.org/10.1038/s43247-022-00498-3

Regmi, S (2021) *Gaussian Smoothing in Time Series Data. Towards Data Science*. Retrieved April 27, 2022, from https://towardsdatascience.com/gaussian-smoothing-in-time-series-data-c6801f8a4dc3

Serreze, M. C., & Barry, R. G. (2011). *Processes and impacts of Arctic amplification: A research synthesis. Global and Planetary Change*, 77(1–2), 85–96. Retrieved March 22, 2022.

Smedsrud, L. H., Esau, I., Ingvaldsen, R. B., Eldevik, T., Haugan, P. M., Li, C., Lien, V. S., Olsen, A., Omar, A. M., Otterå, O. H., Risebrobakken, B., Sandø, A. B., Semenov, V. A., & Sorokina, S. A. (2013). *The role of the Barents Sea in the Arctic climate system. Rev. Geophys, 51, 415–449. Retrieved* August 26, 2022,

SMHI (2022). *Inversion*. Retrieved May 9, 2022, from https://www.smhi.se/kunskapsbanken/inversion-1.28269

Statistikhjälpen. (n.d.). *Tolka output från regressionsanalys*. Retrieved August 26, 2022, from https://www.stathelp.se/sv/regoutput_sv.html

Sundell, A. (2009). *Guide: Regressionsanalys – SPSS-AKUTEN*. Retrieved August 26, 2022, from https://spssakuten.com/2009/12/21/regressionsanalys-1/

Van Pelt, W.J.J., V.A. Pohjola, R. Pettersson, S. Marchenko, J. Kohler, B. Luks, J.O. Hagen, T.V. Schuler, T. Dunse, B. Noël, and C.H. Reijmer (2019). A long-term dataset of climatic mass balance, snow conditions and runoff in Svalbard (1957–2018). *The Cryosphere*, 13, 2259-2280.

Van Pelt, W.J.J., J. Oerlemans, C.H. Reijmer, V.A. Pohjola, R. Pettersson and J.H. van Angelen (2012). Simulating melt, runoff and refreezing on Nordenskiöldbreen, Svalbard, using a coupled snow and energy balance model. *The Cryosphere*, 6, 641-659.

Zamelczyk, K., Fransson, A., Chierici, M., Jones, E., Meilland, J., & Lødemel, H. H. (2021). *Distribution and Abundances of Planktic Foraminifera and Shelled Pteropods During the Polar Night in the Sea-Ice Covered Northern Barents Sea. Frontiers in Marine Science*. Retrieved August 24, 2022.

Data from:
All-Russian Scientific Research Institute of Hydrometeorological Information - World Data Center (VNIIGMI-WDC) http://meteo.ru/

Svalbard Integrated Arctic Earth Observing System (SIOS), https://sios-svalbard.org/

Appendix

A.1 Lapse rate

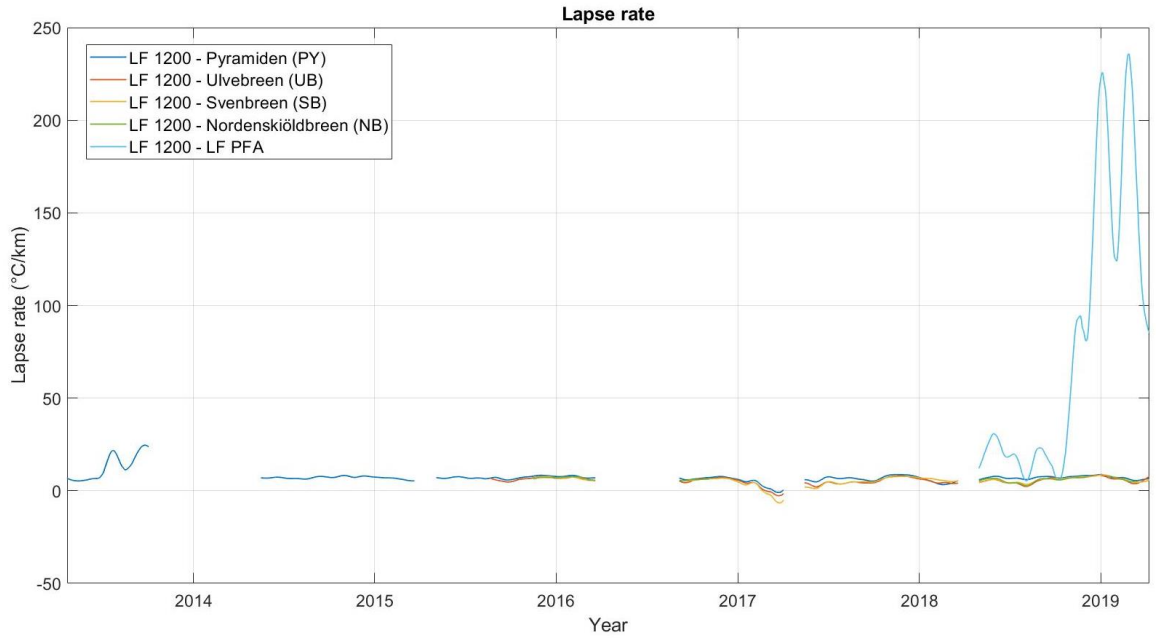

A.1.1 The calculated lapse rate related the highest one Lomonosovfonna 1200 (LF1200), including the Lomonosovfonna PFA (LF PFA) trend and values for 2013. The trends have an applied Gaussian filter.

A.2 Other parameters

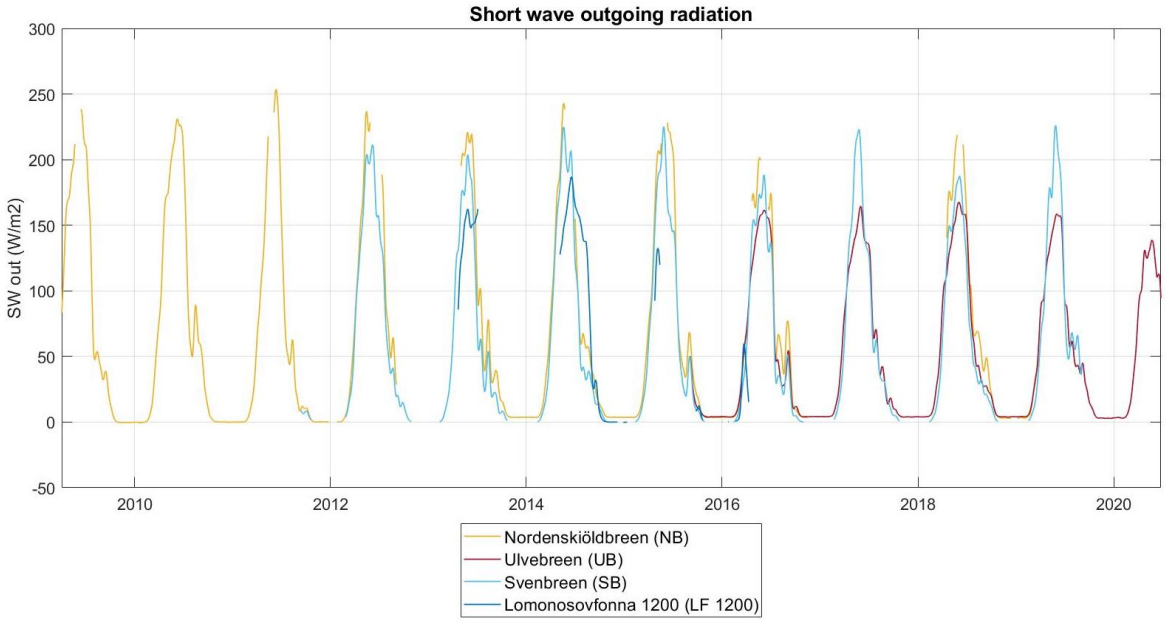

A.2.1 Measured short wave outgoing radiation for all stations, with an applied Gaussian filter.

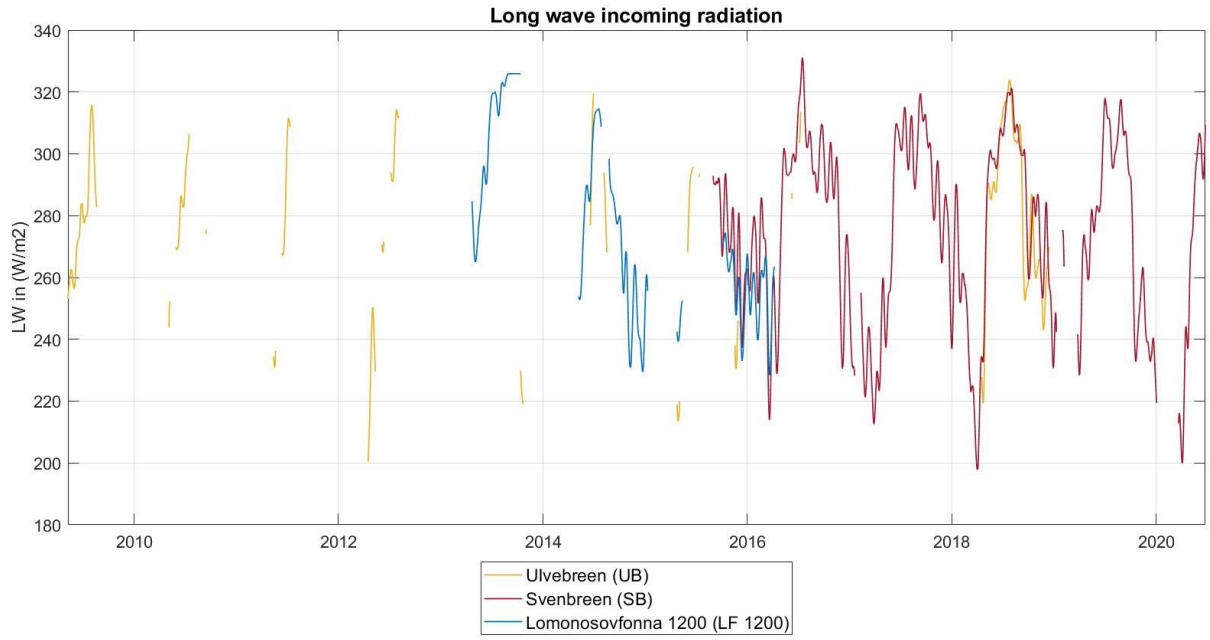

A.2.2 Measured long wave incoming radiation for all stations, with an applied Gaussian filter.

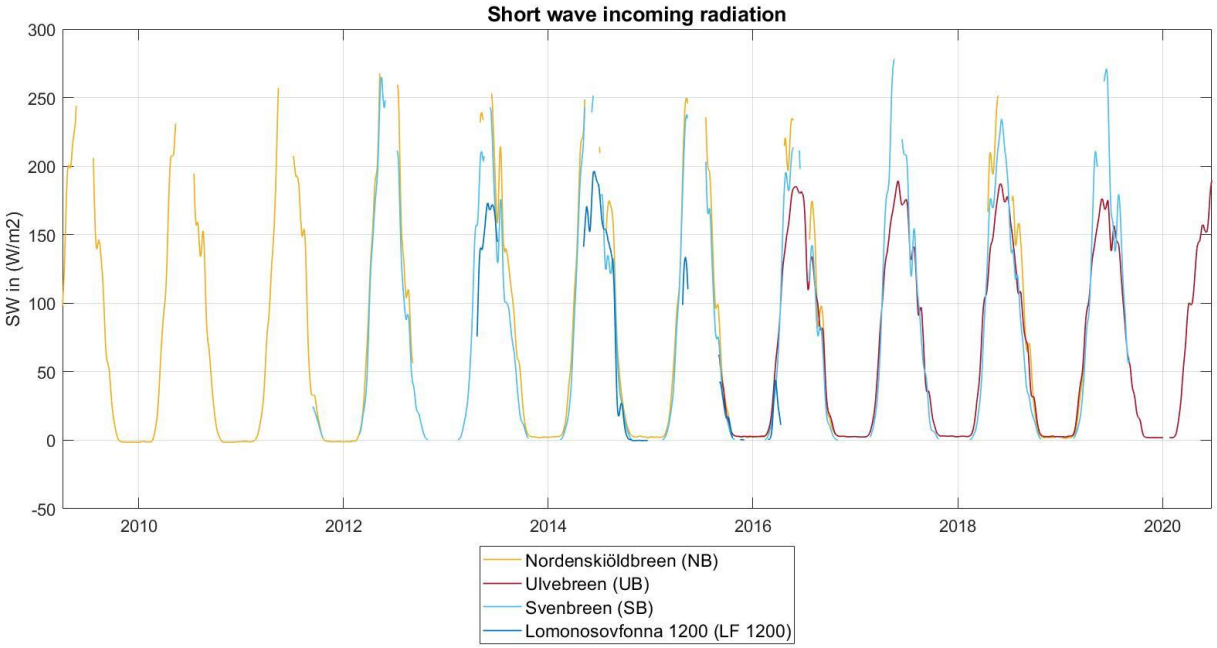

A.2.3 Measured short wave incoming radiation for all stations, with an applied Gaussian filter.

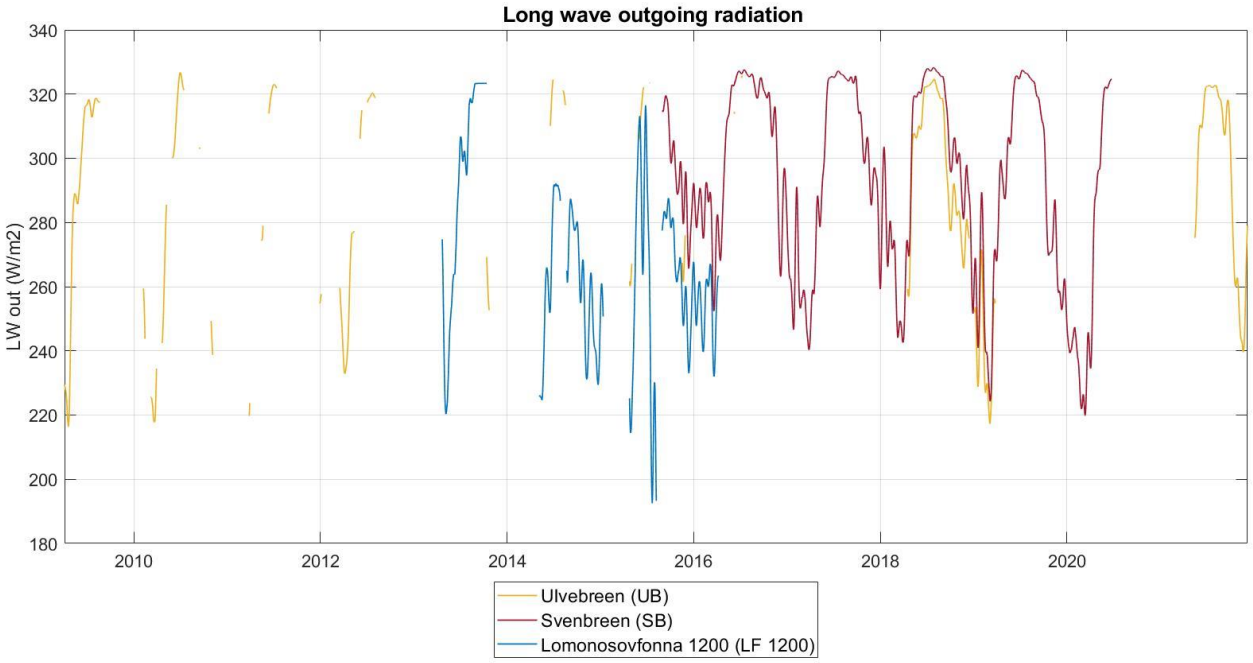

A.2.4 Measured long wave outgoing radiation for all stations, with an applied Gaussian filter.

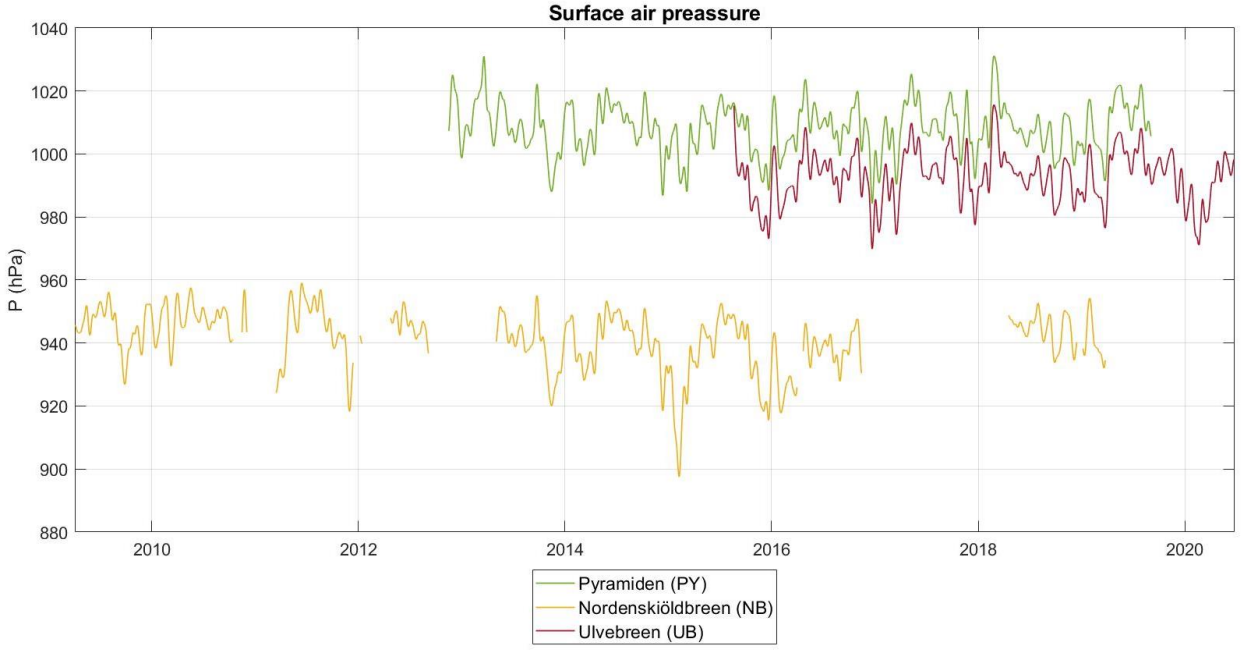

A.2.5 Measured short surface air pressure for all stations, with an applied Gaussian filter.

A.3 Linear regression

A.3.1 Monthly linear regression coefficients for all stations during their entire periods, and its corresponding statistical significance. Since the stations do not have an equal time period, it is not possible to compare them.

Month	FJL			Pyramiden (PY)			Ulvebreen (UB)			Svenbreen (SB)			Nordenskiöldbreen (NB)			Lomonosovfonna PFA (LF_PFA)			Lomonosovfonna 1200 (LF_1200)		
	2000-2017			2012-2019			2015-2020			2011-2019			2009-2019			2018-2020			2013-2019		
	a (ºC/yr)	R^2	P <	*a* (ºC/yr)	R^2	P <	*a* (ºC/yr)	R^2	P <	*a* (ºC/yr)	R^2	P <	*a* (ºC/yr)	R^2	P <	*a* (ºC/yr)	R^2	P <	*a* (ºC/yr)	R^2	P <
Jan	0,448	0,21	0,10	-0,428	0,13	0,44	-1,889	0,55	0,15	-0,543	0,21	0,26	0,090	0,01	0,87	-12,079	NaN	NaN	-0,786	0,21	0,44
Feb	0,537	0,27	0,05	-0,253	0,02	0,79	-2,670	0,83	0,03	-0,176	0,01	0,81	-0,281	0,04	0,66	-13,828	NaN	NaN	0,770	0,07	0,68
Mar	0,525	0,34	0,05	-0,401	0,08	0,53	-2,101	0,81	0,04	-0,659	0,24	0,22	0,081	0,01	0,84	-12,362	NaN	NaN	-1,520	0,54	0,16
Apr	0,393	0,34	0,05	0,352	0,10	0,48	0,116	0,01	0,90	0,463	0,22	0,24	0,368	0,09	0,39	-1,188	0,11	0,79	-0,744	0,21	0,30
May	-0,012	0,00	0,90	0,161	0,02	0,76	-0,151	0,01	0,89	0,150	0,02	0,76	0,037	0,00	0,87	-2,604	0,85	0,25	0,115	0,01	0,86
Jun	-0,029	0,05	0,40	0,130	0,28	0,23	-0,050	0,04	0,74	0,094	0,18	0,30	0,020	0,01	0,77	0,442	NaN	NaN	0,160	0,06	0,70
Jul	0,014	0,04	0,45	0,049	0,02	0,77	-0,058	0,06	0,75	0,183	0,31	0,15	0,044	0,05	0,53	1,386	NaN	NaN	1,847	0,38	0,27
Aug	0,012	0,02	0,65	-0,062	0,04	0,68	0,006	0,00	0,98	-0,009	0,00	0,95	-0,102	0,16	0,26	-1,440	NaN	NaN	0,554	0,23	0,34
Sep	0,187	0,37	0,05	0,337	0,21	0,30	-0,352	0,23	0,33	-0,010	0,00	0,96	-0,137	0,08	0,44	1,392	NaN	NaN	2,955	0,46	0,14
Okt	0,313	0,30	0,05	0,797	0,32	0,25	-1,057	0,31	0,33	0,590	0,36	0,12	-0,020	0,00	0,95	-3,478	NaN	NaN	3,103	0,47	0,13
Nov	0,564	0,30	0,05	1,177	0,62	0,04	-1,071	0,45	0,22	0,716	0,46	0,06	0,158	0,02	0,72	-7,577	NaN	NaN	0,563	0,14	0,54
Dec	0,321	0,14	0,15	0,553	0,53	0,06	-1,113	0,45	0,21	0,335	0,31	0,16	-0,010	0,00	0,97	-11,285	NaN	NaN	0,630	0,26	0,38

A.3.2 Seasonal linear regression coefficients for all stations during their entire periods, and its corresponding statistical significance. Since the stations do not have an equal time period, it is not possible to compare them.

Season	FJL			Pyramiden (PY)			Ulvebreen (UB)			Svenbreen (SB)			Nordenskiöldbreen (NB)			Lomonosovfonna PFA (LF_PFA)			Lomonosovfonna 1200 (LF_1200)		
	2000-2017			2012-2019			2015-2020			2011-2019			2009-2019			2018-2020			2013-2019		
	a (°C/yr)	R^2	P <	*a* (°C/yr)	R^2	P <	*a* (°C/yr)	R^2	P <	*a* (°C/yr)	R^2	P <	*a* (°C/yr)	R^2	P <	*a* (°C/yr)	R^2	P <	*a* (°C/yr)	R^2	P <
Winter	0,284	0,24	0,10	0,166	0,07	0,58	-1,455	0,78	0,05	0,023	0,00	0,92	0,059	0,01	0,80	-10,714	NaN	NaN	-0,239	0,03	0,77
Spring	0,051	0,03	0,55	0,161	0,02	0,76	-0,151	0,01	0,89	0,150	0,02	0,76	0,037	0,00	0,87	-2,604	0,85	0,25	0,115	0,01	0,86
Summer	0,034	0,11	0,25	0,114	0,17	0,37	-0,328	0,88	0,06	0,080	0,10	0,45	-0,044	0,05	0,54	0,445	NaN	NaN	1,365	0,46	0,21
Autumn	0,209	0,13	0,25	0,797	0,32	0,25	-1,057	0,31	0,33	0,590	0,36	0,12	-0,020	0,00	0,95	-3,478	NaN	NaN	2,146	0,36	0,16

A.4 Scatterplot between parameters

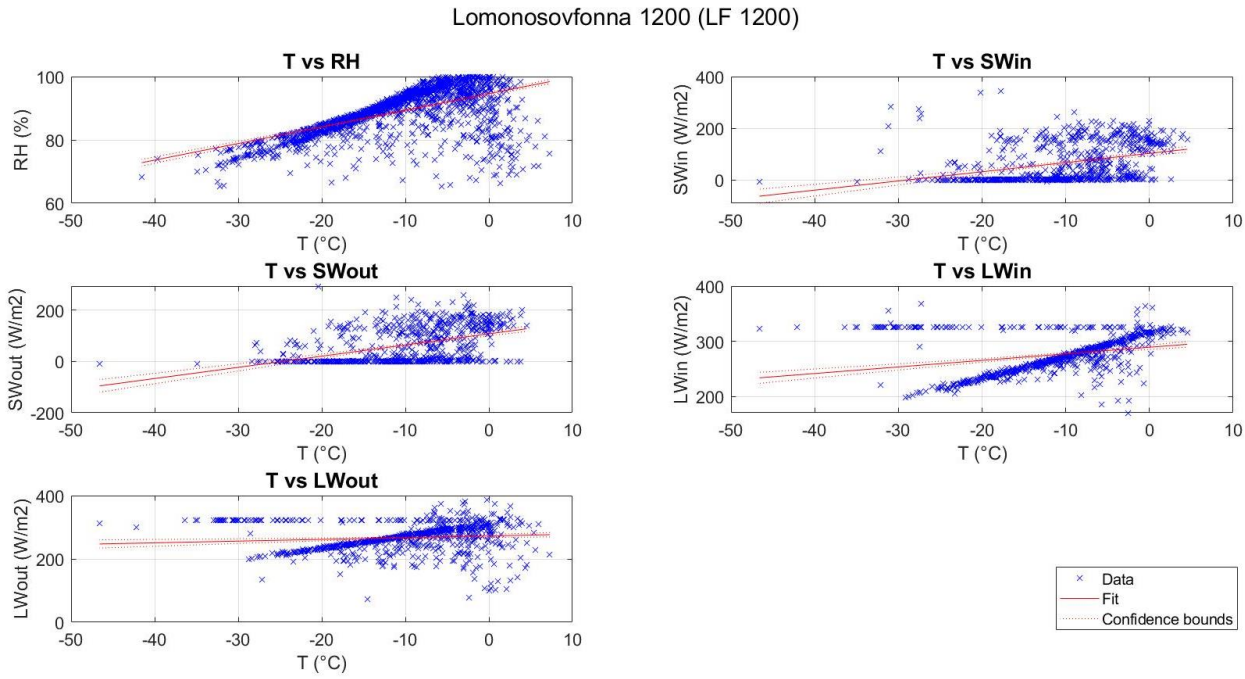

A.4.1 Scatterplots between temperature and other measured parameters for Lomonosovfonna 1200.

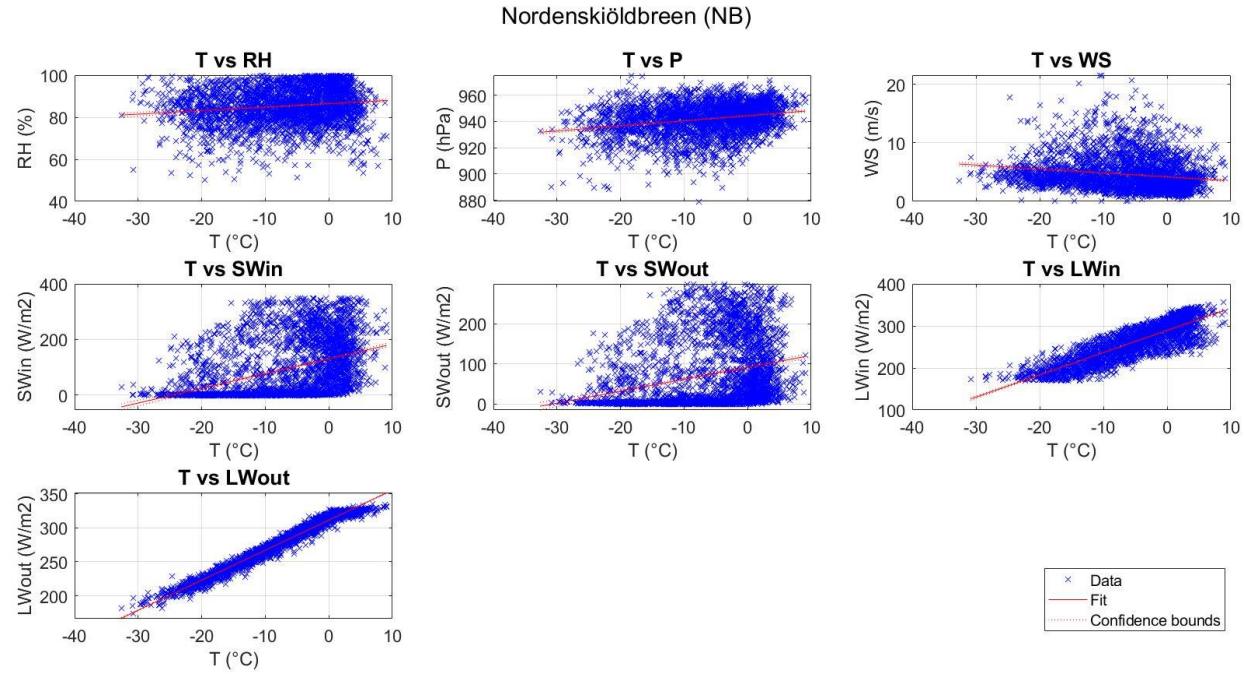

A.4.2 Scatterplots between temperature and other measured parameters for Nordenskiöldbreen.

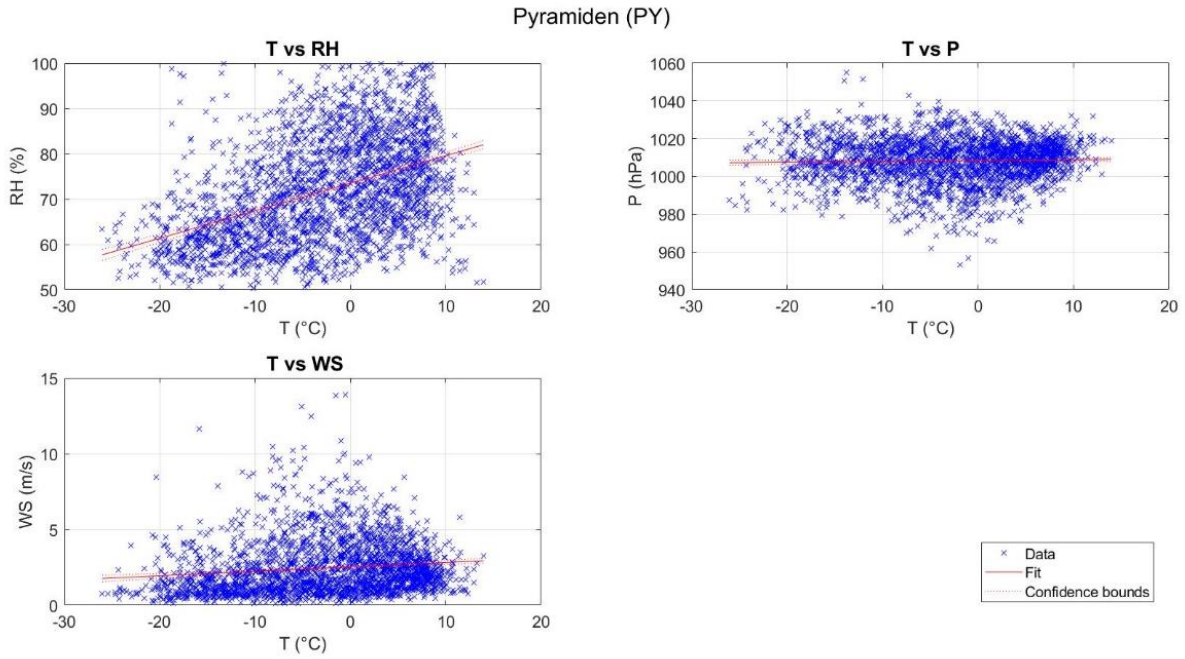

A.4.3 Scatterplots between temperature and other measured parameters for Pyramiden.

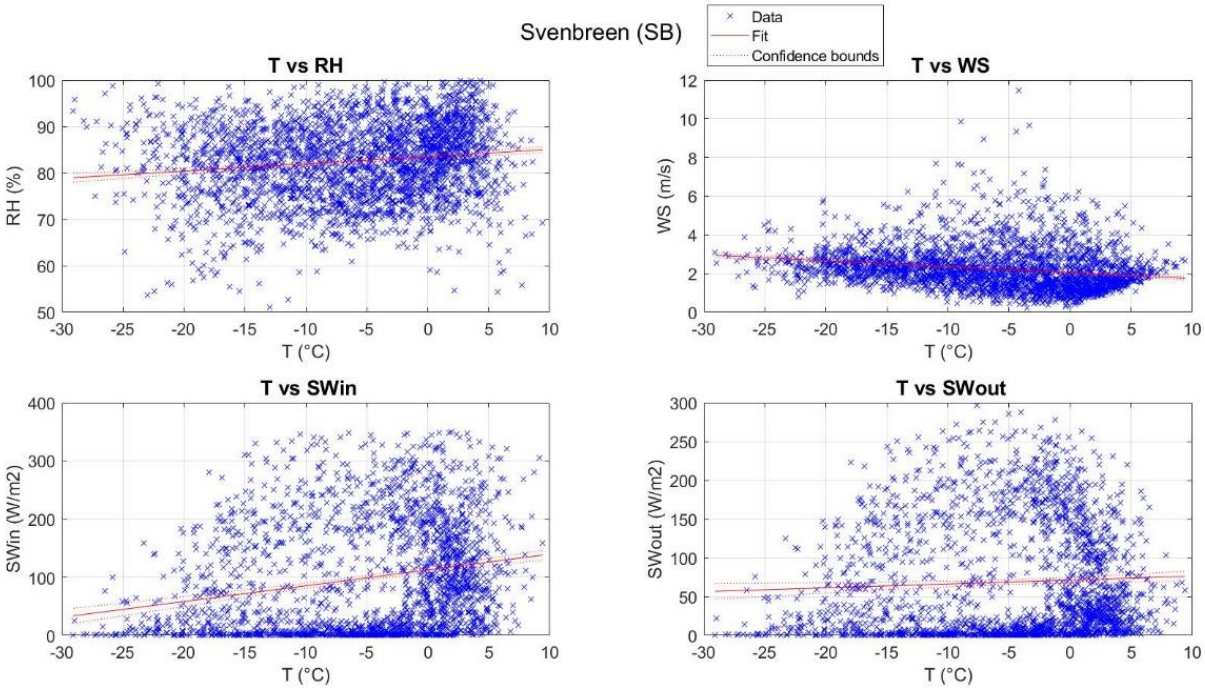

A.4.4 Scatterplots between temperature and other measured parameters for Svenbreen.

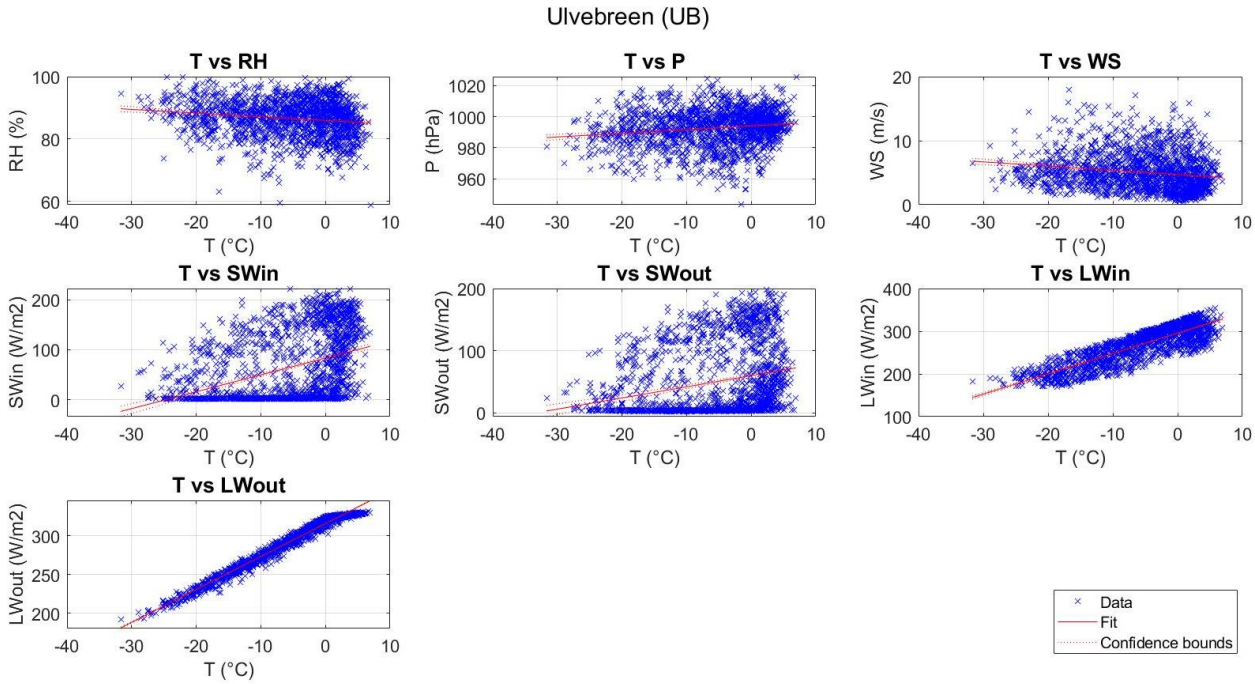

A.4.5 Scatterplots between temperature and other measured parameters for Ulvebreen.